VYSOKÉ UČENÍ TECHNICKÉ V BRNĚ

BRNO UNIVERSITY OF TECHNOLOGY

FAKULTA ELEKTROTECHNIKY A KOMUNIKAČNÍCH TECHNOLOGIÍ

ÚSTAV VÝKONOVÉ ELEKTROTECHNIKY A ELEKTRONIKY

FACULTY OF ELECTRICAL ENGINEERING AND COMMUNICATION

DEPARTMENT OF POWER ELECTRICAL AND ELECTRONIC ENGINEERING

FEA modelling of synchronous machine

DIPLOMOVÁ PRÁCE
MASTER'S THESIS

AUTOR PRÁCE Bc. TIBOR FICZA
AUTHOR

BRNO 2010

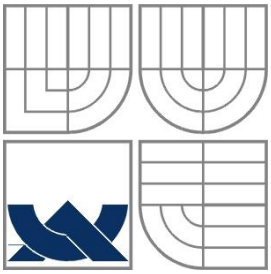

VYSOKÉ UČENÍ TECHNICKÉ V BRNĚ

BRNO UNIVERSITY OF TECHNOLOGY

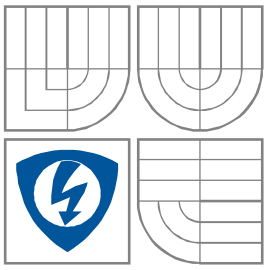

FAKULTA ELEKTROTECHNIKY A KOMUNIKAČNÍCH TECHNOLOGIÍ

ÚSTAV VÝKONOVÉ ELEKTROTECHNIKY A ELEKTRONIKY

FACULTY OF ELECTRICAL ENGINEERING AND COMMUNICATION

DEPARTMENT OF POWER ELECTRICAL AND ELECTRONIC ENGINEERING

Modelování synchronního stroje pomocí MKP

FEA modelling of synchronous machine

DIPLOMOVÁ PRÁCE
MASTER'S THESIS

AUTOR PRÁCE Bc. Tibor Ficza
AUTHOR

VEDOUCÍ PRÁCE doc. Ing. Čestmír Ondrůšek, CSc.
SUPERVISOR

BRNO, 2010

BRNO UNIVERSITY OF TECHNOLOGY

Faculty of Electrical Engineering and Communication

Department of Power Electrical and Electronic Engineering

Diploma thesis

master's study field

Power Electrical and Electronic Engineering

Student: Tibor Ficza, Bc. ***ID:*** 83806

Year of study: 2 ***Akademic year:*** 2009/10

Title of thesis:

FEA modelling of synchronous machine

INSTRUCTION:

1. Provide the literature search.
2. Indentify critical parameters and develop simplified model.
3. Make 2D and 3D models.
4. Evaluate the results.

REFERENCE:

According to supervizor recommendation

Assigment deadline: 1.10.2009 ***Submission deadline:*** 20.5.2010

Head of thesis: doc. Ing. Čestmír Ondrůšek, CSc.

Consultant: Ing. Rostislav Huzlík

doc. Ing. Čestmír Ondrůšek, CSc.

Subject Council Chairman

Abstract

This work disserts with FEA modeling of synchronous machines with surfaced permanent magnets on his rotor. Firstly, we are choosing our machine what we want to model, in our case it is a three-phase synchronous machine with permanent magnets on its rotor from the company VUES-Brno. First, I have calculated the parameters of the machine then I have made static model of our machine . Next, I was trying to find out possibilities how to make dynamic model or animation of this machine through the use of program FEMM and Matlab. Then I will made 3D model and simulate our machine in Ansys Workbench.

Keywords

Synchronous machine, PM, model, FEMM, magnetic flux, density, permeability, air gap, current, voltage.

Anotácia

Táto práca sa zaoberá s modelovaním synchronného stroja s permanentnými magnetmi pomocou metody konečných prvkov. K modelovaniu sme si zvolili 3 fázový synchronný stroj s permanentnými magnetmi na povrchu rotora z firmy VUES. Najprv vypočítame parametre stroja a potom spravíme statický model pomocou programu FEMM a Matlab a budeme hladať možné riešenia na 2D dynamický model. Pomocou programu Ansys Workbench spravíme 3D model tohoto stroja budeme a porovnávať výsledky simulácií.

Kľúčové slová

Synchrónny stroj, PM, magnetický tok, reaktancia, vzduchová medzera, MKP

Bibliografic citation

FICZA, T. *FEA modelling of synchronous machine*. Brno: Vysoké učení technické v Brně, Fakulta elektrotechniky a komunikačních technologií, 2010. 51 pages.Vedoucí diplomové práce doc. Ing. Čestmír Ondrůšek, CSc.

Prehlásenie (Statement)

Prehlasujem, že svoju diplomovú prácu na tému „FEA modeling of synchronous machine“ som vypracoval samostatne pod vedením vedúceho semestrálneho projektu a s použitím odbornej literatúry a dalších informačních zdrojov, ktoré sú všetky citované v práci a uvedené v zoznamu literatúry na konci práce.

Ako autor uvedenej diplomovej práce ďalej prehlasujem, že v súvislosti s vytvorením tejto diplomovej práce som neporušil autorské práva tretích osôb, predovšetkým som nezasiahol nedovoleným spôsobom do cudzích autorských práv osobnostných a som si plne vedomí následkov porušenia ustanovení § 11 a nasledujúcich autorského zákona č. 121/2000 Sb., vrátane možných trestnoprávných dôsledkov vyplývajúcich z ustanovení § 152 trestného zákona č. 140/1961 Sb.

V Brne dňa …… Podpis autora ……..

Acknowledgments

Thanks are due to doc. Ing. Čestmír Ondrůšek, CSc. and Ing. Rostislav Huzlík for the motivation, professional help and hints in creating this work.

SUMMARY

INDEX OF FIGURES

INDEX OF TABLES

INDEX OF CHARTS

DEFINITION AND MEASURE OF USED SYMBOLS

B	-	magnetic flux density (T)
I	-	electric current (A)
N	-	number of coil turns (-)
S	-	area (m^2)
g	-	air gap (m)
i_m	-	magnetic current (A)
l	-	lenght (m)
Φ	-	magnetic flux (Wb)
θ	-	angle (˚)
μ_r	-	relative permeability (-)
X''_d	-	subtrainsent reactances (Ω)
X'_d	-	transient reactances (-)
X_a	-	mutual reactances (-)
X_s	-	synchronous reactances (-)
ns	-	synchronous speed (rpm)
T	-	torque (Nm)
σ_{Ftan}	-	avarage tangetial stress (Pa)
A	-	linear current density (kA/m)
q	-	number of slots per pole and phase (-)
y_Q	-	slot pitches (-)
k_C	-	Carter factor (-)
t_1	-	slot pitch (m)
τ	-	pole pitch (m)
τ_{d1}	-	leakage factor (-)
λ_{1s}	-	leakage permeance (-)
λ_{1d}	-	differential leakage flux (-)
ϕ	-	magntic flux(Wb)

INTRODUCTION

This diploma thesis is dealing with FEA modeling of synchronous machine with permanent magnets on his rotor. In this work I am modeling a particular machine which was designed by the company VUES-Brno. First, I would like to explain why are these types of machines so important. Permanent magnet ac motors have the advantage of not requiring any magnetising current in his rotor. Hence, they can operate at a higher power factor and efficiency than an induction motor in the fractional to 30 kW region. So, there is a big effort to design more efficient and stronger machines of this construction with good control properties to enable their wider use in different kinds of ways.

Firstly, I provide the literature search and then identify the critical parameters. For the simulation with finite element method I have chosen program FEMM, which is possible to download free from the internet. It is easy to use for 2D static models with wide range of options and possibilities and this program is collaborating with program Matlab. Finite element method is an effective and relatively fast method for solving all boundary problems described by differencial equations.

In the second part I have chosen program Ansys Workbench and I was making a 3D model. With this program 3D case can be modeled and it is more effective than program FEMM and the results are more accurate.

1 FEA MODELING

1.1 Finite Element Method

The basic design of an electrical machine, that is the dimensioning of the magnetic and electric circuits, is usually carried out by applying analytical equations. However, accurate performance of the machine is usually evaluated by using different numerical methods. With these numerical methods, the effect of a single parameter on the dynamical performance of the machine can be effectively studied.

The most widely used numeric method is the finite element method (FEM or FEA) which can be used for the analysis of two- or three-dimensional electromagnetic field problems. The solution can be obtained for static, time-harmonic or transient problems. In the latter two cases, the electric circuit describing the power supply of the machine is coupled with the actual field solution. When applying FEM in the electromagnetic analysis of an electrical machine, special attention has to be paid to the relevance of the electromagnetic material data of the structural parts of the machine as well as to the construction of the finite element mesh. Because most of the magnetic energy is stored in the air-gap of the machine and important torque calculation formulations are related to the air-gap field solution, the mesh has to be sufficiently dense in this area. The rule is that the air-gap mesh should be divided at least into three layers to achieve accurate results. In the transient analysis, that is, in time-stepping solutions, the selection of the size of the time step is also important in order to include the effect of high-order time harmonics in the solution. A common method is to divide one time cycle at least into 400 steps, but the division could be even denser then this, in particular with highspeed machines.

1.2 FEMM

FEMM is a suite of programs for solving low frequency electromagnetic problems on two-dimensional planar and axisymmetric domains. The program currently addresses linear/nonlinear magnetostatic problems, linear/nonlinear time harmonic magnetic problems, linear electrostatic problems, and steady-state heat flow problems. FEMM is divided into three parts:

• Interactive shell (femm.exe). This program is a Multiple Document Interface pre-processor and a post-processor for the various types of problems solved by FEMM. It contains a CAD-like interface for laying out the geometry of the problem to be solved and for defining material properties and boundary conditions. Autocad DXF files can be imported to facilitate the analysis of existing geometries. Field solutions can be displayed in the form of contour and density plots.

The program also allows the user to inspect the field at arbitrary points, as well as evaluate a number of different integrals and plot various quantities of interest along user-defined contours.

• triangle.exe. Triangle breaks down the solution region into a large number of triangles, a vital part of the finite element process. This program was written by Jonathan Shewchuk and is available from his Carnegie-Mellon University.

• Solvers (fkern.exe for magnetics; belasolv for electrostatics); hsolv for heat flow problems; and csolv for current flow problems.. Each solver takes a set of data files that describe problem and solves the relevant partial differential equations to obtain values for the desired field throughout the solution domain.

2 PARAMETERS OF SMPM MACHINE

2.1 Sketch of the stator and rotor

Synchronous motors operate at a constant speed in absolute synchronism with the line frequency. Synchronous motors are classified according to their rotor's design, construction, materials and operation into the four basic groups:

- electromagnetically-excited motors
- PM motors
- reluctance motors
- hysteresis motors

In electromagnetically excited and PM motors a cage winding is frequently mounted on salient-pole rotors to provide asynchronous starting and to damp oscillations under transient conditions, so-called *damper winding.* Developments in rare-earth PM materials and power electronics have opened new prospects on the design, construction and application of PM synchronous motors. Servo drives with PM motors from static inverters are finding applications on an increasing scale.

The surface magnet motor can have magnets magnetized radially or sometimes circum ferentially. An external high conductivity nonferromagnetic cylinder can be used in some cases. It protects the PMs against the demagnetizing action of armature reaction and centrifugal forces, provides an asynchronous starting torque, and acts as a damper. If rare-earth PMs are used, the synchronous reactances in the *d*- and q-axis are practically the same, as in my case.

As stated at the beginning, the model will be a 6 pole three-phase synchronous machine with permanent magnets on the rotor wich was designed by the company VUES Brno. I obtained only the sketch of the stator (Fig. 1) and a rotor (Fig. 2) without any other parametrs from the company. So the other calculations and parametrs like stator windings, power factor and efficiency are selected and calculated by me. The sketch of given SMPM machine is shown below.

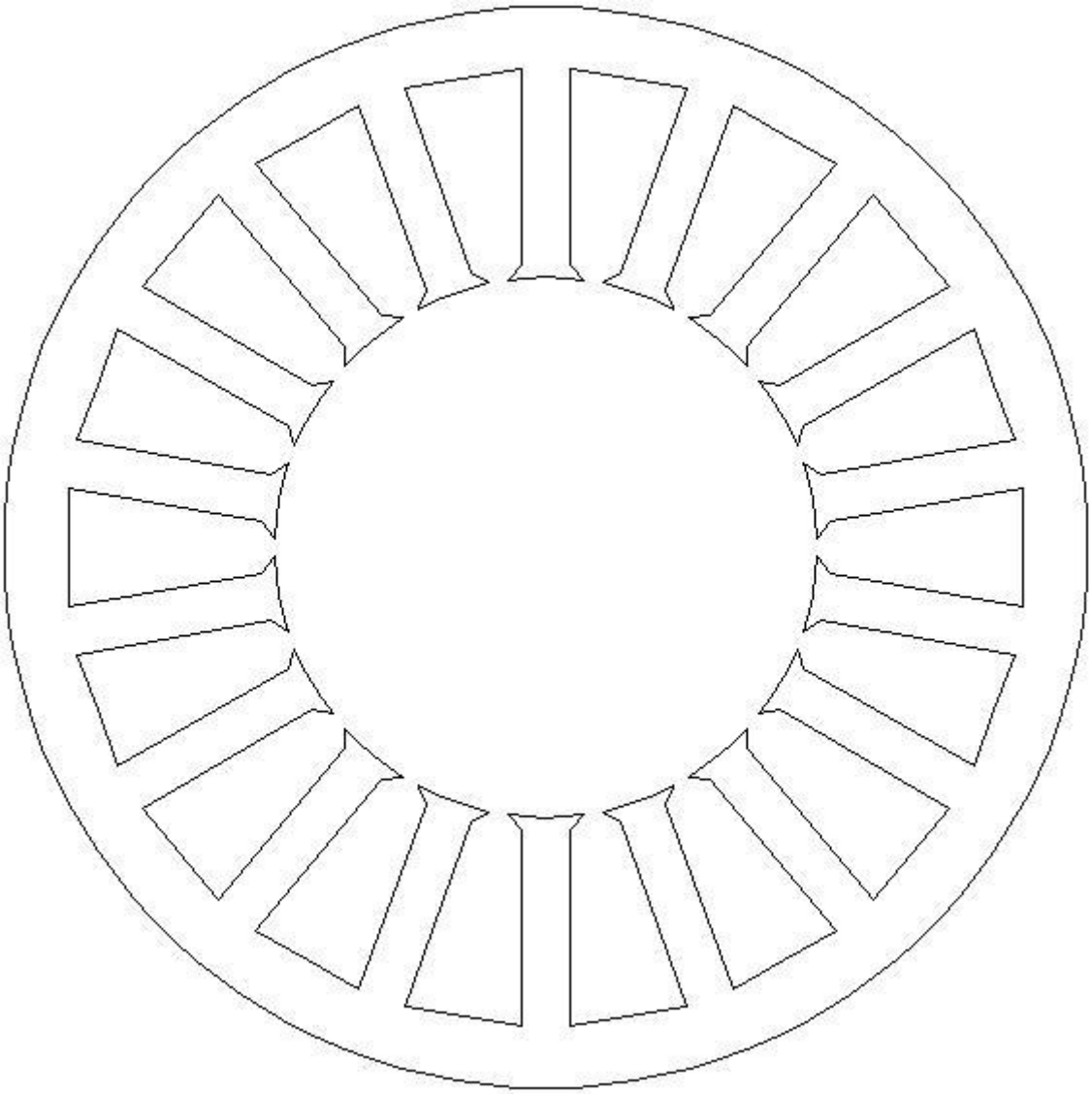

Fig. 1 Sketch of the stator

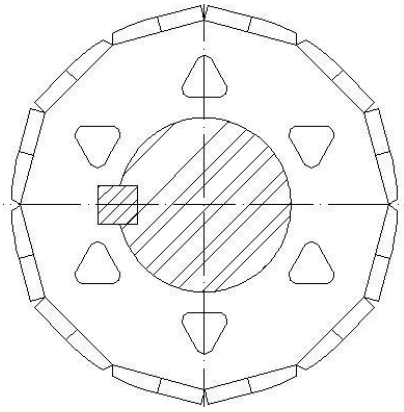

Fig. 2 Sketch of the stator

2.2 Calculating the parameters of the machine

From the sketch can be seen that the model has:

18 slots and 6 poles.

Next, the speed of the rotating magnetic field of the stator is calculated:

$$n_s = \frac{120.f}{p} = \frac{120.50}{6} = 1000\ rpm \qquad (2.1)$$

where ***p*** is the number of poles, ***f*** is the frequency of electrical power network.

Now, the possible minimal and maximal torque (2.2) can be calculated. This tangential stress produces the torque of the machine when acting upon the rotor surface. Typical tangential stress values from Table 1.0, give the starting point for the torque parameters of the machine. There are three stress values, calculated with the lowest linear current density and flux density, with the average values and with the highest values. The flux density and linear current density distributions are assumed to be sinusoidal. The power factor of synchronous machines is assumed to be 1. When the size of the rotor is known, the suitable tangential stress value on the rotor surface from Table 1.0, then the torque value can be obtained as:

$$T = 2.\sigma_{Ftan}.r_r.S_r = 2.\sigma_{Ftan}.2.\pi.r_r^2.l' = 2.\sigma_{Ftan}.V_r \qquad (2.2)$$

where $\boldsymbol{\sigma_{Ftan}}$ is the average tangential stress value on the surface, $\boldsymbol{r_r}$ is the rotor radius, ***l'*** is the rotor equivalent length and $\boldsymbol{S_r}$ is the rotor surface facing the air-gap.

	Sailent-pole synchronous machines or PMSMs
A/kA/m,RMS	36-65
Air-gap flux density $\widehat{B_{\delta 1}}/T$	0.85-1.05
Tangential stress σ_{Ftan}/PA	
minimum	21000*
average	33500*
maximum	48000*
	*cos φ = 1

Table 1- Typical tangencial stress values

$$T_{min} = 21000.\pi.\frac{0.0616^2\ .\ 0.127}{2} = 15.89 \cong 16Nm$$

$$T_{max} = 48000.\pi.\frac{0.0616^2\ .\ 0.127}{2} = 36.33 \cong 38Nm$$

Now, the following parameters of synchronous machine are chosen:

A=50 kA/m

U_s=400V => U_f=230 V

cos φ=1

$\eta = 0{,}9$

T=16-38 Nm

J=5 A/mm^2

So, aware of this data, the number of winding turns in one slot and the diameter of the coil, regarding to the minimal and the maximal torque, can be determined.

<u>With the minimal torque the calculation of the current and the number of winding turns is:</u>

$$P_2 = M.\omega = M.2.\pi.n = 16.2.\pi.16{,}67 = 1675{,}85\ W \qquad (2.3)$$

$$P_1 = \frac{P_2}{\eta} = \frac{1675{,}85W}{0{,}9} = 1862{,}05\ W \qquad (2.4)$$

$$I = \frac{P_1}{3.U_f \cos\varphi} = \frac{1862{,}05}{3.230.1} = 2{,}69A \qquad (2.5)$$

$$N_S = \frac{A.\pi.D}{2.I.m} = \frac{50000.\pi.0{,}063}{2.2{,}69.3} = 613{,}136\ turns\ per\ phase \qquad (2.6)$$

$$Z_Q = \frac{N_S.2.m}{Q_S} = \frac{613{,}136.2.3}{18} = 204{,}378\ turns\ per\ slot \qquad (2.7)$$

$$J = \frac{I}{S} => S = \frac{I}{J} = \frac{2{,}69}{5} = 0{,}538\ mm^2 \qquad (2.8)$$

<u>d=0,82 mm</u>

With the maximum torque the calculating of the current and the number of winding turns is:

$$P_2 = M.\omega = M.2.\pi.n = 38.2.\pi.16{,}67 = 3980{,}14\ W$$

$$P_1 = \frac{P_2}{\eta} = \frac{3980{,}14W}{0{,}9} = 4422{,}38\ W$$

$$I = \frac{P_1}{3.U_f \cos\varphi} = \frac{4422{,}38}{3.230.1} = 6{,}409\ A$$

$$N_S = \frac{A.\pi.D}{2.I.m} = \frac{50000.\pi.0{,}063}{2.6{,}409.3} = 257{,}346\ turns\ per\ phase$$

$$Z_Q = \frac{N_S.2.m}{Q_S} = \frac{257{,}346.2.3}{18} = 85{,}782\ turns\ per\ slot$$

$$J = \frac{I}{S} => S = \frac{I}{J} = \frac{6{,}409}{5} = 1{,}2818\ mm^2$$

d=1,2775 mm

Later, in the model the diameter of coil was set to 1.25mm.

P_{2n}	Minimum output power	[kW]	1,675
P_{2max}	Maximal output power	[kW]	3,980
V_{nom}	Nominal supply voltage	[V]	230
I_{min}	Phase current	[A]	2,690
I_{max}	Phase current	[A]	6,409
p	Number of poles	[-]	6
m	Number of phases	[-]	3
n_n	Rated speed	[rpm]	1000
T_{min}	Minimal torque	[Nm]	16
T_{max}	Maximum torque	[Nm]	38

Table 2 - Main parameters of analyzed PM synchronous machine

2.3 Phase windings

Now, the calculation of the number of slots for each such zone by ***q*** , as a number of slots per pole and phase is following:

$$q = \frac{Q}{2.p_p.m} \qquad (2.9)$$

Here, ***Q*** is the number of slots in the stator, ***m*** is number of phase and ***pp*** is the number of pole pairs.

$$q = \frac{18}{2.3.3} = 1$$

The coil span is expressed in the number of slot pitches y_Q:

$$y_Q = \frac{Q}{2.p} = 3$$

Placement of the coils in the stator winding of the machine can be seen in Fig. 3. It displays all the 18 slots. **A** is beginning and $\mathbf{A_0}$ is the end of the coil. In the work, the ends are are assumed to be connected, so it is a star connection machine. Current flowing through one coil of one phase is one quarter of nominal current because of the number of parallel paths.

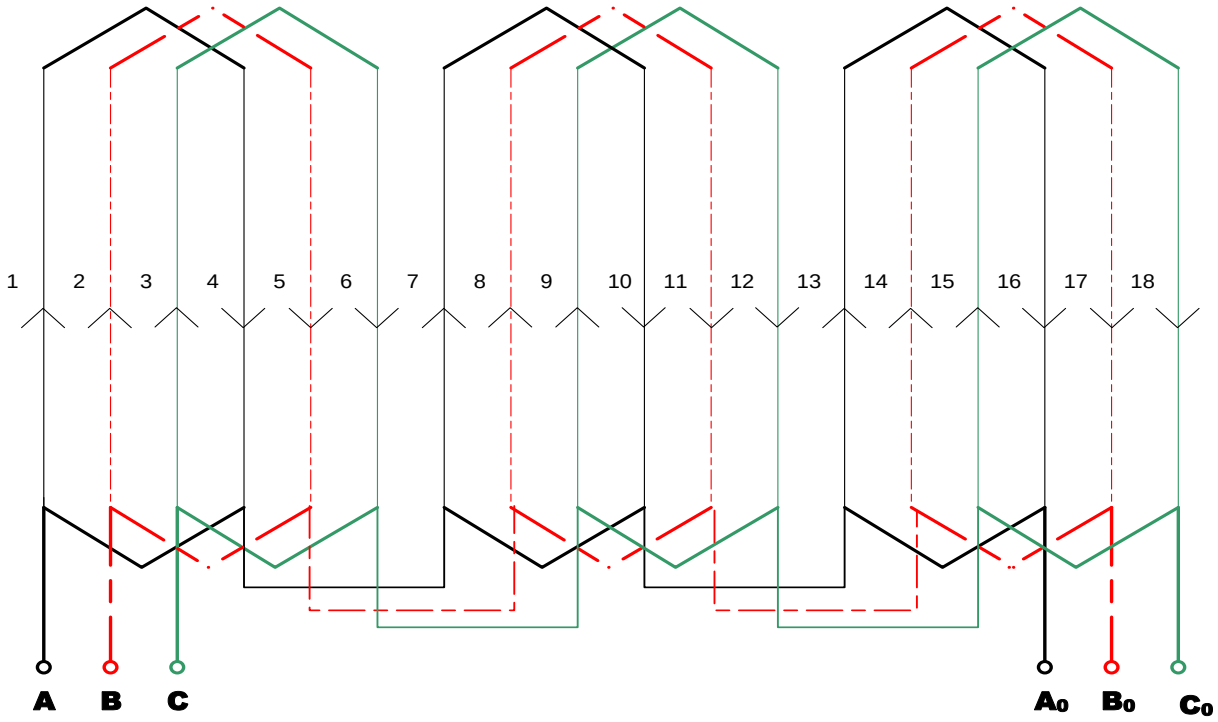

Fig. 3 Placement of the coils in the winding

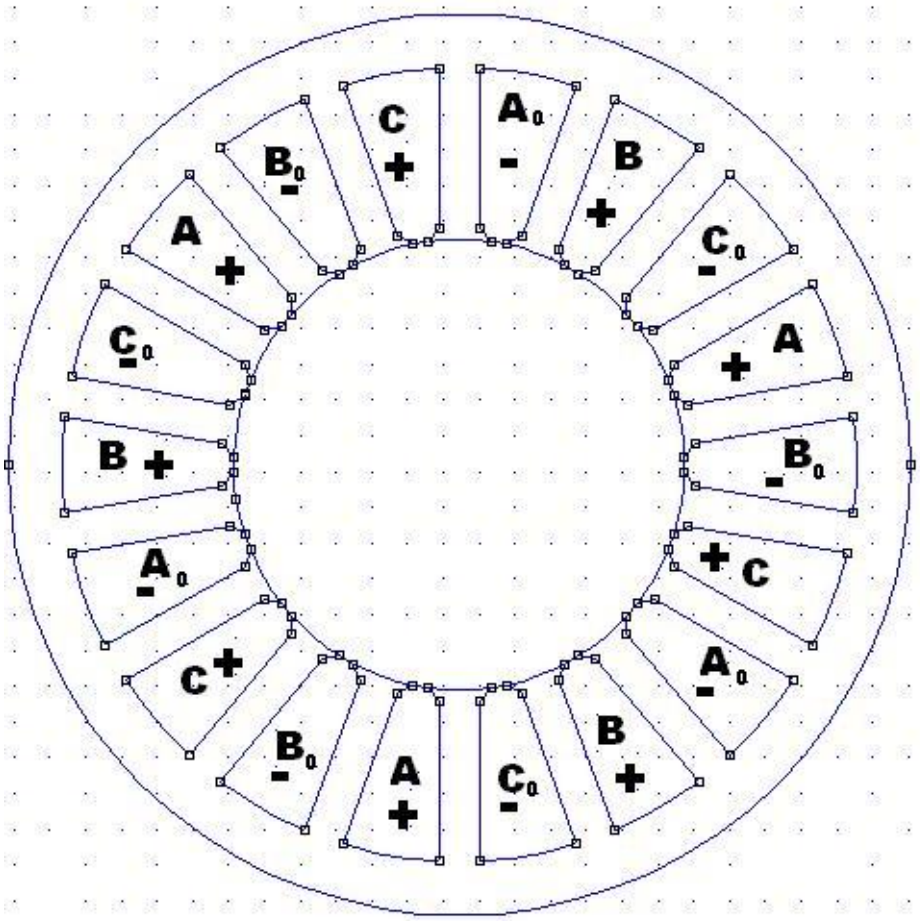

Fig. 4 Division of the periphery of a three-phase, six-pole machine into phase zones of positive and negative values

3 DESIGNING THE MODEL IN FEMM

First of all, it is necessary to draw the machine in AutoCAD, then it can be imported to FEMM. One advantage of the FEMM is, that is has CAD-like interface. Firstly, the new magnetic problem is set up, then the DXF file can be loaded. After that, the main parameters , in the problem definitions. So, the problem type I set up to planar, lenght units will be in millimeters, the frequency is let on zero. The depth will be 76 and the solver precicion is 1e-008. During setting the conditions, a proper choice of the elements was taken into account, so the surface can be better described by the mesh with the expected magnetic inductance. On the other hand, there was an effort to make the mesh not so soft since the computation of the model could last much longer time. In the case of magnetic circuit of a synchronous machine it is necessary to increase the density of the mesh in places where the gradients of magnetic induction are big, like stator and rotor slots, the edges in air gaps, and air gaps as well. In the surface of the air gap the size of the element was chosen in order to have 4 elements on the width of air gap.(Fig. 5) The area of air gap and the part of the iron is meshed by soft mesh so we get the necessary amount of data for the graph of distribution of magnetic induction in the air gap. The surface of the magnets was divided into 4 parts and on each surface I set the materails of the magnets. By this I managed to get a more realistic simulation of magnetic flux lines.

Some discussion about the boundary conditions is neccesary, to make sure how to define an adequate number of boundary conditions to guarantee a unique solution.

Boundary conditions for magnetic and electrostatic problems come in some varieties, but in this work the *Dirichlet-type* conditions will be assumed. In this type of boundary condition, the value of potential A or V is explicitly defined on the boundary, *e.g.* $A = 0$. The most common use of Dirichlet-type boundary conditions in magnetic problems is to define $A = 0$ along a boundary to keep magnetic flux from crossing the boundary. In electrostatic problems, Dirichlet conditions are used to fix the voltage of a surface in the problem domain.

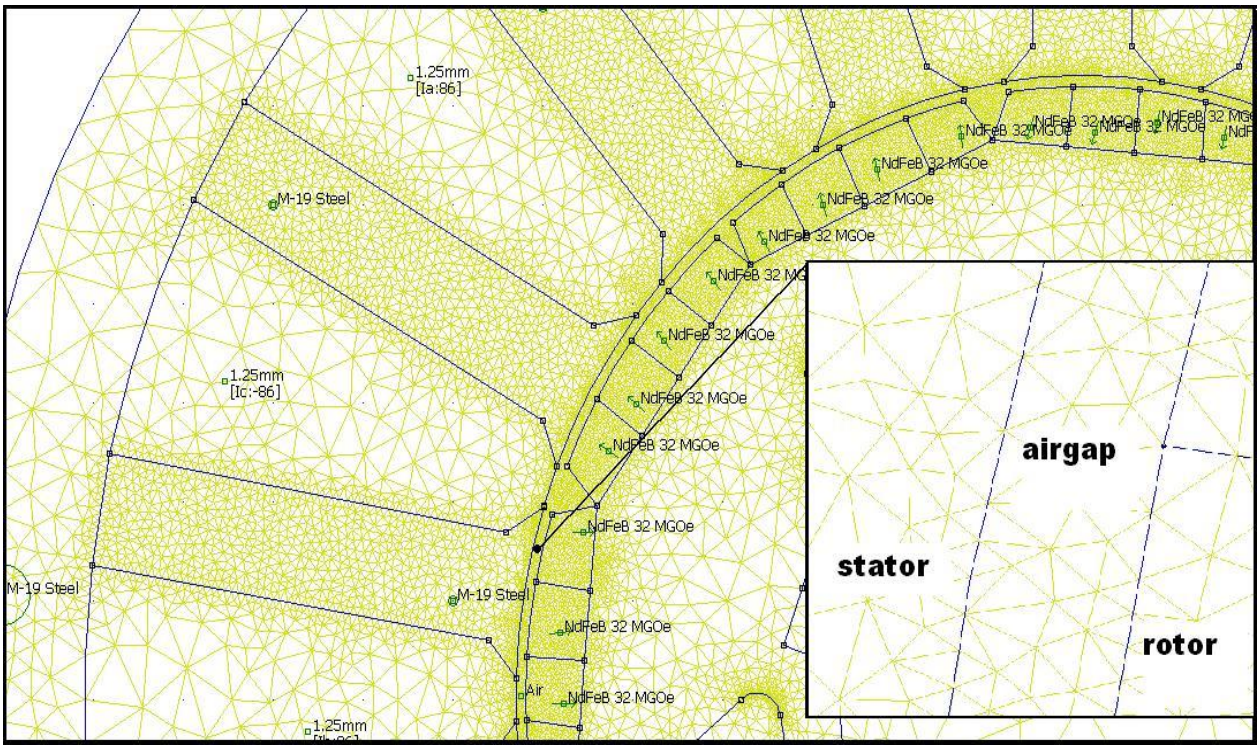

Fig. 5 The mesh elements in the model

3.1 Charateristics of material

3.1.1 Material of magnets

NdFeB-NEODYMIUM IRON BORON MAGNETS

Known as third generation of Rare Earth magnets, Neodymium Iron Boron (NdFeB) magnets are the most powerful and advanced commercialized permanent magnets today. Since they are made from Neodymium, one of the most plentiful rare earth elements, and inexpensive iron, NdFeB magnets offer the best value in cost and performance.

H_c	Remanence	[kA/m]	915
B_r	Coercive force	[T]	1,24
αB	Temperature coefficient of B	[-]	-0,11
αH	Temperature coefficient of H	[-]	-0,51
T	Operating temperature	[degC]	70
HcT	Coercive force at T	[kA/m]	681,7
BrT	Remanence at T	[T]	1,17
μ_r	Recoil permability	[-]	1,08

Table 3 - Parameters of NdFeB magnet

3.1.2 Material of steel

When low carbon steel is alloyed with small quantities of silicon, the added volume resistivity helps to reduce eddy current losses in the core. Silicon steels are probably of the most use to designers of motion control products where the additional cost is justified by the increased performance. These steels are available in an array of grades and thicknesses so that the material may be tailored for various applications. The added silicon has a marked impact on the life of stamping tooling, and the surface insulation selected also affects die life. Silicon steels are generally specified and selected on the basis of allowable core loss in watts/lb. M numbers, such as M19, M27, M36 or M43, with each grade specifying a maximum core loss. M19 is probably the most common grade for motion control products, as it offers nearly the lowest core loss in this class of material, with only a small cost impact, particularly in low to medium production quantities.

Material	Properties
Iron sheet	B-H curve
Copper	μr=0.99999
Air	μr=1.00000

Table 4 - Material properties

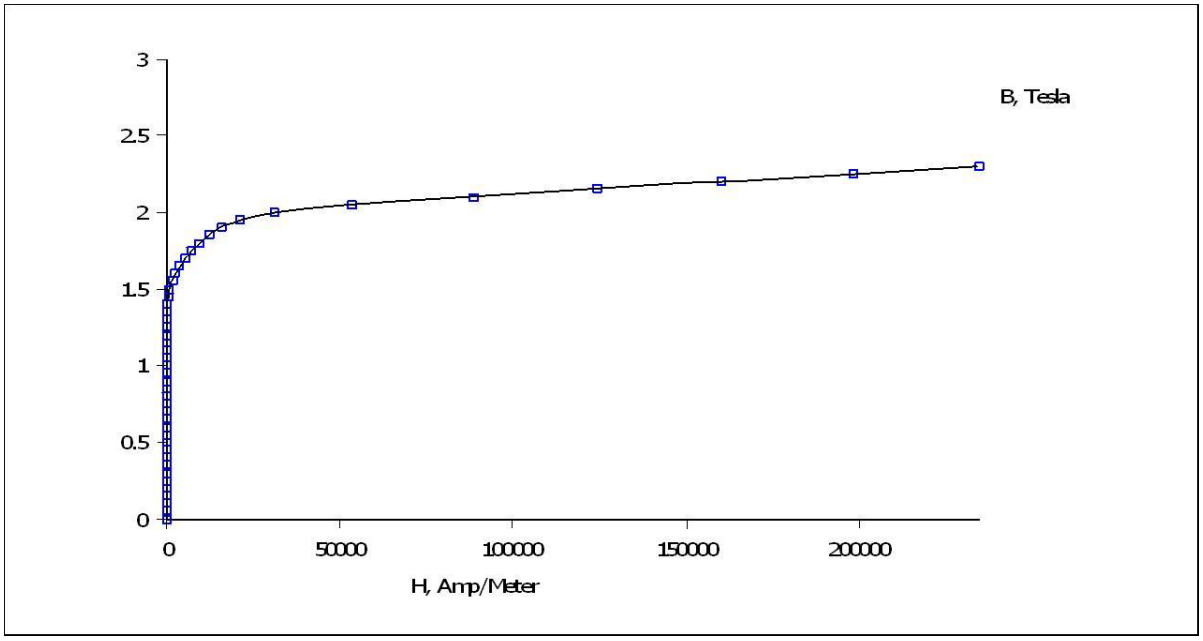

Fig. 6 B-H curve of M-19 steel

4 CRITICAL PARAMETERS

Transient phenomenona in synchronous machines are generating by the rapid changes in the working process, for example cable connection to the electrical power net and disconnecting from it, fast change in load, at short-circuit, etc. These phenomenona in synchronous machines may have effect on the stability of machines, i.e. on the ability to keep the synchronous speed at the change of steady-state performance. The ability to predict the subtransient reactance of a particular generator design is of prime importance. Power system designers routinely use the generator subtransient reactance as a key parameter to aid in the design of the complete electrical power generation system.

The subtransient reactance, $\boldsymbol{X''_d}$, is the generator internal impedance element that is effective in the first cycles of a transient load event and determines the magnitude of the instantaneous fault current from the generator. The transient reactance, $\boldsymbol{X'_d}$, becomes effective after approximately 6 cycles into a transient load event and determines the amount of voltage change seen at the generator terminals due to the step change in load. As stated, the reactances of a generator have a direct effect on the transient fault currents experienced in an electrical power generation system, as well as the motor starting capability of the generator. The magnitudes of the fault currents need to be calculated so that breakers, etc. can be sized accordingly. The peak magnitudes of the three-phase fault currents are inversely proportional to the subtransient reactance of the generator. For new generator designs, the transient and subtransient reactances are routinely tested as part of a thorough evaluation of the generator's performance characteristics.

The accuracy of calculating the steady-state performance of small permanent magnet (PM), synchronous motors depends on the accuracy of calculating the synchronous reactances in the *d*- and *q* - axes. For typical medium power and large synchronous motors with electromagnetic excitation analytical methods using form factors of the stator (armature) magnetic flux density are good enough. Small PM synchronous motors sometimes have a complicated structure, and numerical or analog modeling is necessary to obtain an accurate distribution of the magnetic field. This distribution is very helpful to correctly estimate the form factors of the rotor and stator magnetic flux densities.

As it is known, the d- and q-axes synchronous reactances are defined as (1) :

$$X_{sd} = X_{ad} + X_1 \qquad (4\text{–}1) \qquad X_{sq} = X_{aq} + X_1 \qquad (4.2)$$

where $\boldsymbol{X_{ad}}$ is the *d*-axis mutual (armature reaction) reactance, $\boldsymbol{X_{aq}}$ is the *q*-axis mutual reactance, and $\boldsymbol{X_1}$ is the armature winding leakage reactance per phase. The reactance $\boldsymbol{X_{ad}}$ and sometimes $\boldsymbol{X_{aq}}$ depend on the magnetic saturation due to the main flux. The leakage reactance $\boldsymbol{X_1}$

consists of the slot, differential, tooth–top, and end-connection leakage reactances. Only the slot and differential leakage reactances depend on the magnetic saturation due to leakage fields. It can be taken into account using Norman's method. The analytical approach for calculating the synchronous reactances is based on the distribution of the stator winding normal component magnetic flux density. This distribution can be assumed to be a periodic function of the stator inner perimeter or can be found using numerical or analog modeling. The *d*-axis mutual reactance and *q*-axis mutual reactance are expressed in terms of form factors of the stator field (armature reaction factors) $\boldsymbol{k_{fd}}$ and $\boldsymbol{k_{fq}}$

$$X_{ad} = k_{fd} \cdot X_a \qquad (4.3) \qquad X_{aq} = k_{fq} \cdot X_a \qquad (4.4)$$

The mutual reactance $\boldsymbol{X_a}$ is the same as that for a cylindrical rotor synchronous machine

$$X_a = 4.m.\mu_0.f \cdot \frac{(N_1.k_{w1})^2}{\pi.p} \cdot \frac{\tau.L_i}{k_c.g} \qquad (4.5)$$

where $\boldsymbol{m_1}$ is the number of stator (armature) phases, $\boldsymbol{\mu_0}$ is the permeability of free space, $\boldsymbol{f}$ is the input frequency,$\boldsymbol{N_1}$ is the number of stator turns per phase, $\boldsymbol{k_{w1}}$ is the stator winding factor for the fundamental space harmonic, $\boldsymbol{p}$ is the number of pole pairs,$\boldsymbol{\tau}$ is the pole pitch ,$\boldsymbol{L_i}$ is the effective length of the armature core, $\boldsymbol{k_C}$ is Carter's coefficient for the airgap, and $\boldsymbol{g}$ is the airgap in the *d*-axis. To obtain a saturated synchronous reactance, the equivalent airgap $\boldsymbol{k_C g}$ should be multiplied by the saturation factor $k_{sat}>1$ of the magnetic circuit, i.e., to obtain $\boldsymbol{k_C k_{sat} g}$. In most salient pole synchronous machines with electromagnetic excitation, the magnetic saturation affects only $\boldsymbol{X_{sd}}$ since the *q*-axis airgap is comparatively very large. In some PM synchronous machines the magnetic saturation affects both $\boldsymbol{X_{sd}}$ and $\boldsymbol{X_{sq}}$. The form factors of the stator field are defined from tabulated funds. $k_{fd}=1$ and $k_{fq}=1$.

4.1 Subtransient synchronous reactance

The d-axis subtransient synchronous reactance is defined for generator operation, for the first instant of a sudden short circuit of the stator, when the damper and the excitation winding, if it exists, repel the armature magnetic flux. The same effect appears for motoring, when the rotor is suddenly locked. The subtransient synchronous reactance is the sum of the stator winding leakage reactance $\boldsymbol{X_1}$ and the parallel connection of the reactances of the damper $\boldsymbol{X_{damp}}$, field excitation winding $\boldsymbol{X_{exc}}$ and the d-axis armature reaction reactance.

(4.6)

$$X_d^{''} = X_1 + \frac{1}{\frac{1}{X_{ad}} + \frac{1}{X_{exc}} + \frac{1}{X_{damp}}}$$

(4.7)

$$X_q^{''} = X_1 + \frac{1}{\frac{1}{X_{aq}} + \frac{1}{X_{exc}} + \frac{1}{X_{damp}}}$$

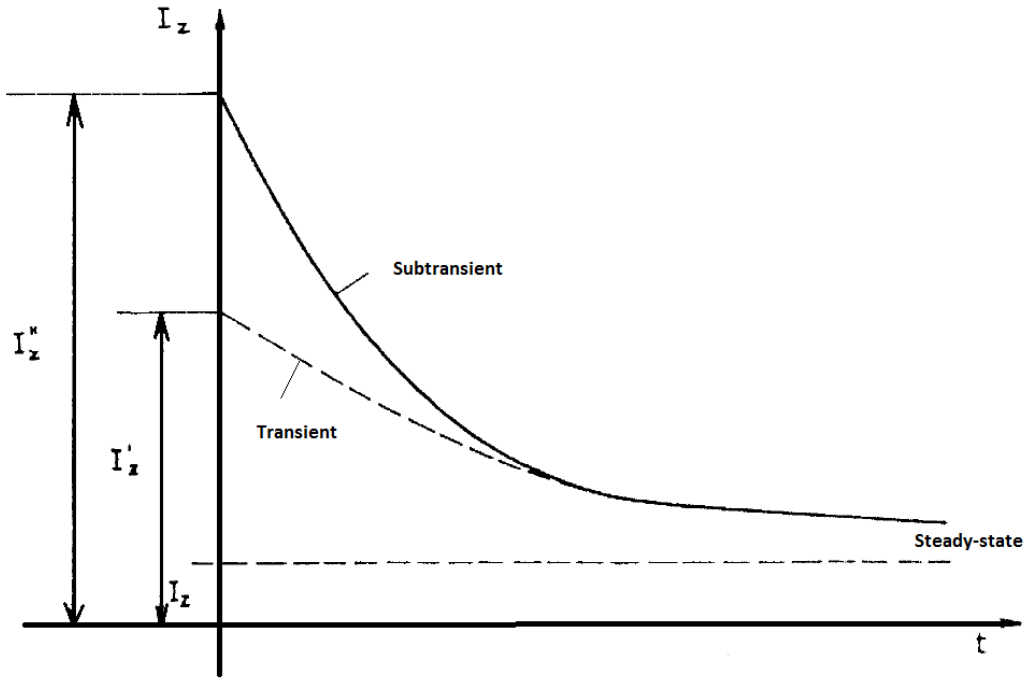

Fig. 7 Curve of the short-circuit currents in synchronous machines

4.2 Transient synchronous reactance

With the exponential decay of the damping-winding current, the armature MMF is able to force its flux deeper into the pole (despite the opposition of the induced rotor current). The decay of the current in the excitation winding is slower than that in the damper since the inductance of the excitation winding is larger. This stage is characterized by the transient reactance.

(4.8)

$$X_d^{'} = X_1 + \frac{1}{\frac{1}{X_{ad}} + \frac{1}{X_{exc}}}$$

(4.9)

$$X_q^{'} = X_1 + \frac{1}{\frac{1}{X_{aq}} + \frac{1}{X_{exc}}}$$

In practice very often used , like in my case, where the function of the damper winding is overlaying the massive rotor, in case with cylindrical rotor or the massive pole and pole shoe of the sailent pole machine. Transient actions in these machines is proceeding approximately in the same way like in machines with damper windings, but the damping ability of massive rotors or poles are however principle weaker. Smaller synchronous machines sometimes are producing without damper windings. Their transient actions are described with above-mentioned formula with the difference, that all marked terms by two strokes are falling off. So in my case, it will be only the transient equations.

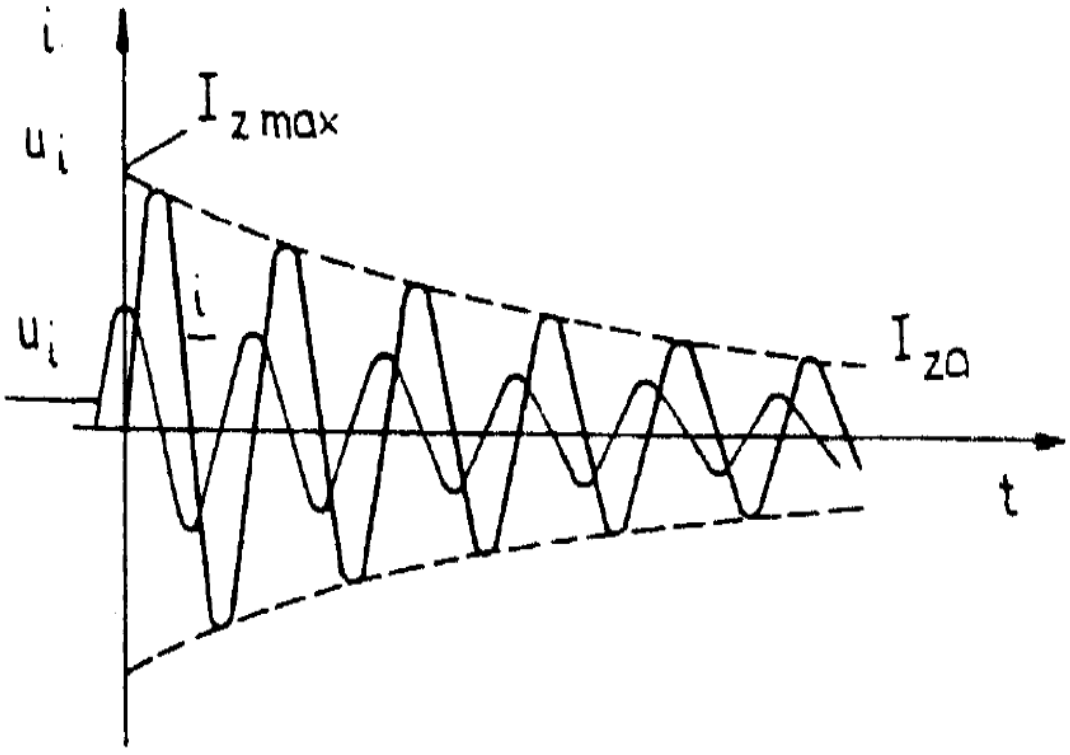

Fig. 8 Curve of symmetric short-circuit current

4.3 Synchronous reactance calculation

First, the slot leakage permeance is calculated from the shape of the slot. Formula below is typical for semi-closed trapezoidal slot.

$$\lambda_{1s} = \frac{h_{11}}{3.b_{12}} \cdot k_t + \frac{h_{12}}{b_{12}} + \frac{2.h_{13}}{b_{12}+b_{14}} + \frac{h_{14}}{b_{14}} = \frac{20}{3.6} \cdot 0{,}92 + \frac{2{,}5}{6} + \frac{2.1}{6+2{,}2} + \frac{0{,}5}{2{,}2} = 1{,}91 \quad (4.10)$$

$$t = \frac{b_{11}}{b_{12}} = \frac{13{,}8}{6} = 2{,}3 \quad (4.11)$$

$$k_t = 3 \cdot \frac{4.t^2 - t^4.(3 - 4.ln.t) - 1}{4.(t^2-1)^2.(t-1)} = 3 \cdot \frac{4.2{,}3^2 - 2{,}3^4.(3 - 4.ln.2{,}3) - 1}{4.(2{,}3^2-1)^2.(2{,}3-1)} = 0{,}92 \quad (4.12)$$

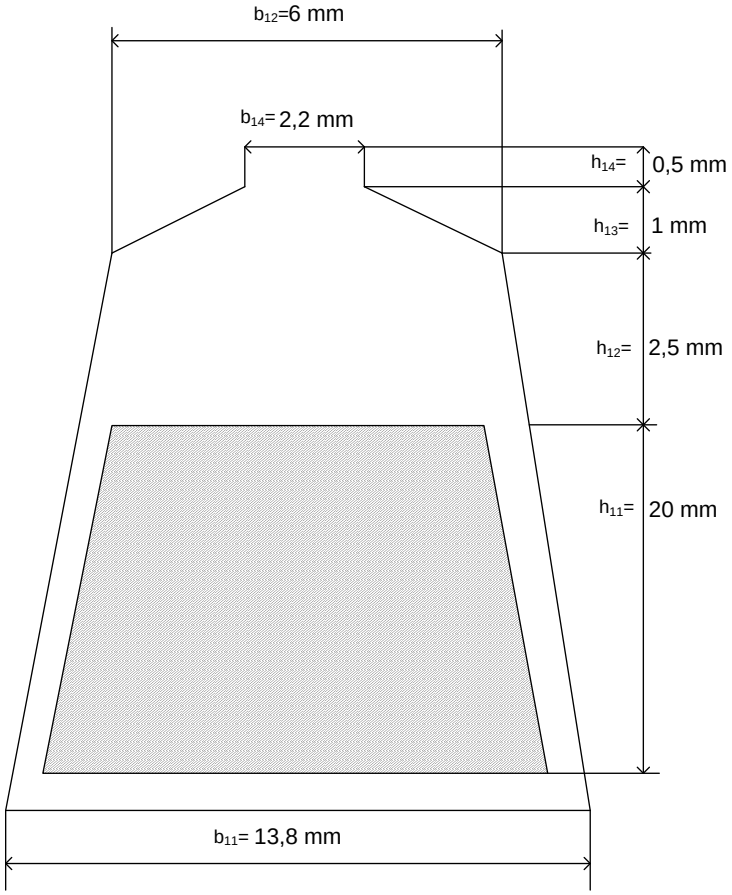

Fig. 9 Shape of the trapezoidal stator slot¨

The tooth-top specific permeance (between the heads of teeth) is*:* *(4.13)*

$$\lambda_{1t} = \frac{5.g/b_{14}}{5 + 4.g/b_{14}} = \frac{5.1{,}7/2{,}2}{5 + 4.1{,}7/2{,}2} = 0{,}7203$$

The specific permaence of the differential leakage flux is

(4.14)

$$\lambda_{1d} = \frac{m_1.q_1.\tau.k_{w1}^2}{\pi^2.g.k_c.k_{sat}} \cdot \tau_{d1} = \frac{3.18.0{,}0329.0{,}96^2}{\pi^2.1{,}5.1{,}026.1} \cdot 1{,}1932 = 0{,}1288$$

where the differential leakage factor $\boldsymbol{\tau_{d1}}$ can be calculated with the following formula

(4.15)

$$\tau_{d1} = \left[\frac{\pi^2.(10.q_1^2+2)}{27}.sin\frac{30^\circ}{q_1}\right] - 1 = \left[\frac{\pi^2.(10.1^2+2)}{27}.sin\frac{30^\circ}{1}\right] - 1 = 1{,}1932$$

End connection leakage permeance, where $\boldsymbol{h_{1t}}$ is the heigth of the stator tooth, $\boldsymbol{l_{1e}}$ is the lenght of a single end connection for cylindrical machine is

(4.16)

$$l_{1e} \approx (0{,}083p + 1{,}217).\frac{p.D_{1n} + h_{1t}}{2.p} + 0{,}02 == (0{,}083.3 + 1{,}217) \cdot \frac{3.0{,}063 + 0{,}048}{2.3} + 0{,}02$$

$$== 0{,}0779$$

$\boldsymbol{q_1}$=q=1 is the number of slot per pole per phase, so the end connection leakage permeance with single-layer windigs will be

(4.17)

$$\lambda_{1e} = 0{,}2 \cdot q_1 = 0{,}2 \cdot \frac{z_1}{2.p.m} = 0{,}2 \cdot \frac{18}{2.3.3} = 0{,}2\ m$$

The pole pitch is:

(4.18)

$$\tau = \frac{\pi.D_{1in}.}{2.p} = \frac{\pi.0{,}063}{2.3} = 0{,}0329\ m$$

where $\boldsymbol{D_{1n}}$ is the stator diameter.

Carter's coefficient for the resultant air gap in the d-axis is

(4.19)

$$g_t = g_q - d_p = 4{,}4 - 3{,}5 = 0{,}9\ mm$$

then Carter's factor is

(4.20)

$$k_c = \frac{t_1}{t_1 - \gamma_1.g_t} = \frac{10{,}995}{10{,}995 - 0{,}3157.0{,}9} = 1{,}026$$

where the slot pitch is

(4.21)

$$t_1 = \frac{\pi.D_{1n}}{z_1} = \frac{\pi.0{,}063}{18} = 0{,}010995\ m$$

and

(4.22)

$$\gamma_1 = \frac{4}{\pi} \cdot \left[\frac{b_{14}}{2.g} \cdot arctan\left(\frac{b_{14}}{2.g}\right) - ln\sqrt{1+\left(\frac{b_{14}}{2.g}\right)^2} \right] =$$

$$= \frac{4}{\pi} \cdot \left[\frac{2{,}2}{2.1{,}5} arctan\left(\frac{2{,}2}{2.1{,}5}\right) - ln\sqrt{1+\left(\frac{2{,}2}{2.1{,}5}\right)^2} \right] = 0{,}3157$$

the equivalent air gap $\boldsymbol{g'}$ in d-axis should be replaced by:

(4.23)

$$g' = g.k_c.k_{sat} + \frac{h_m}{\mu_{rrec}} = 1{,}5 \cdot 1{,}04 \cdot 1 + \frac{3{,}5}{1{,}0784} = 4{,}8055$$

where *(4.24)*

$$\mu_{rrec} = \frac{B_r}{\mu_0 \cdot H_c} = \frac{1{,}24}{0{,}4 \cdot \pi \cdot 10^{-6} \cdot 915000} = 1{,}0784$$

the equivalent air gap $\boldsymbol{g'_q}$ in q-axis should be replaced by *(4.25)*

$$g'_q = g_q.k_c.k_{satq} = 4{,}4.1{,}026.1 = 4{,}51$$

the thickness of the mild steel pole shoe is: *(4.26)*

$$c'_g = 1 - \frac{d_p}{g_q} = 1 - \frac{3{,}5}{4{,}4} = 0{,}2045$$

So now, the d-axis armature reaction reactance, $\boldsymbol{X_{ad}}$, can be calculated, also called d-axis mutual reactance, and than $\boldsymbol{X_{aq}}$, the q-axis armature reaction reactance, also called q-axis mutual reactance. The reactance $\boldsymbol{X_{ad}}$ is sensitive to the saturation of the magnetic circuit while the influence of the magnetic saturation on the reactance $\boldsymbol{X_{aq}}$ depends on the rotor construction. In salient-pole synchronous machines with electromagnetic excitation ***Xaq*** is practically independent of the magnetic saturation.

(4.27)

$$X_{ad} = 4.m.\mu_0.f \cdot \frac{(N_1.k_{w1})^2}{\pi.p} \cdot \frac{\tau.L_i}{g'} = 4.3.0{,}4.\pi.10^{-6}.50 \cdot \frac{(258.0{,}96)^2}{\pi.3} \cdot \frac{0{,}03298.0{,}151}{0{,}0048055} =$$

$$= 5{,}085\Omega$$

(4.28)

$$X_{aq} = 4.m.\mu_0.f \cdot \frac{(N_1.k_{w1})^2}{\pi.p} \cdot \frac{\tau.L_i}{g'_q} = 4.3.0{,}4.\pi.10^{-6}.50 \cdot \frac{(258.0{,}96)^2}{\pi.3} \cdot \frac{0{,}03298.0{,}151}{0{,}00451} =$$

$$= 5{,}419\Omega$$

The leakage reactance is*:* *(4.29)*

$$X_1 = 4.\pi.\mu_0.f \cdot \frac{N^2.L_i}{p.q} \cdot \left[\lambda_{1s} + \frac{l_{1e}}{L_i} \cdot \lambda_{1e} + \lambda_{1d} + \lambda_{1t}\right] =$$

$$= 4.\pi.0{,}4.\pi.10^{-6}.50 \cdot \frac{258^2.0{,}151}{3.1} \cdot \left[1{,}91 + \frac{0{,}0779}{0{,}151} \cdot 0{,}2 + 0{,}1080 + 0{,}7203\right] =$$

$$= 7{,}51\ \Omega$$

So finally, the synchronous reactances in d-axes and q-axes are obtained:

(4.30)

$$X_{sd} = X_1 + X_{ad} = 7{,}51 + 5{,}085 = 12{,}595\Omega$$

(4.31)

$$X_{sq} = X_1 + X_{aq} = 7{,}51 + 5{,}419 = 12{,}929\Omega$$

The stable short-circuit current is

(4.32)

$$I_{za} = \frac{\sqrt{2}.U_f}{X_d} = \frac{\sqrt{2}.230}{12{,}85} = 25{,}83\ A$$

5 RESULTS OF THE SIMULATION IN FEMM

5.1 Simulation without currents and winding

First, I have made simulation of the model without currents in the stator windings. From the analyse it can be seen how the magnetic fulx lines are closing in the machine. Furthermore, also the simulation shows that the magnetic flux is concentrating to the teeth of the stator. The magnetic flux density in teeth achieving values around 1,49 T, or from value 1,3T to 1,49T. In the air gap the magnetic flux density is moving around values 0,7 - 1,0 T. In the edges of the teeth we can remark occuring oversaturating, where the magnetic flux density reaches values around 2,2 T, it is caused by sharp shaped teeth and its small surface. On Fig. 14 it can be seen how is changing the cogging tourque without currents in air gap and reaches maxuimum value 1,5 Nm. Fig. 15. is showing the sinusoidal shape of fluxlinkage in the air gap. On the next figure, a very good influence of stator slots to the shape of the magnetic flux density of the machine is shown.

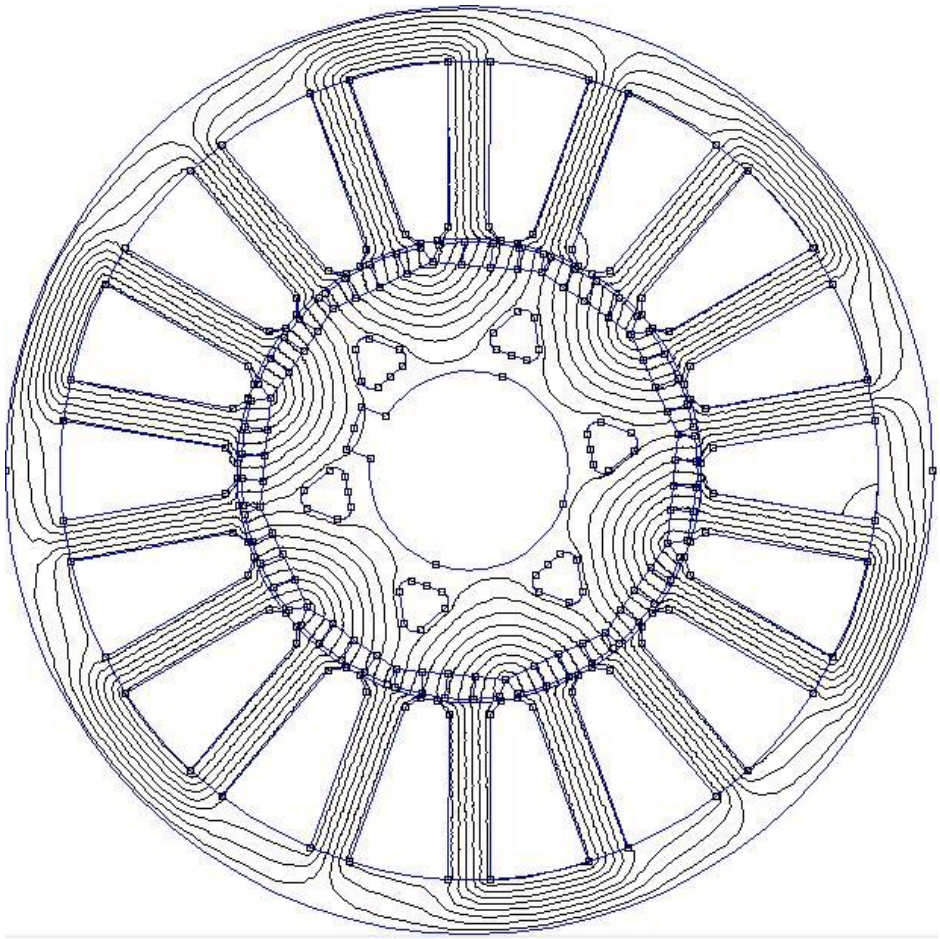

Fig. 10 Flux lines in 3-phase 6 pole synchronous machine

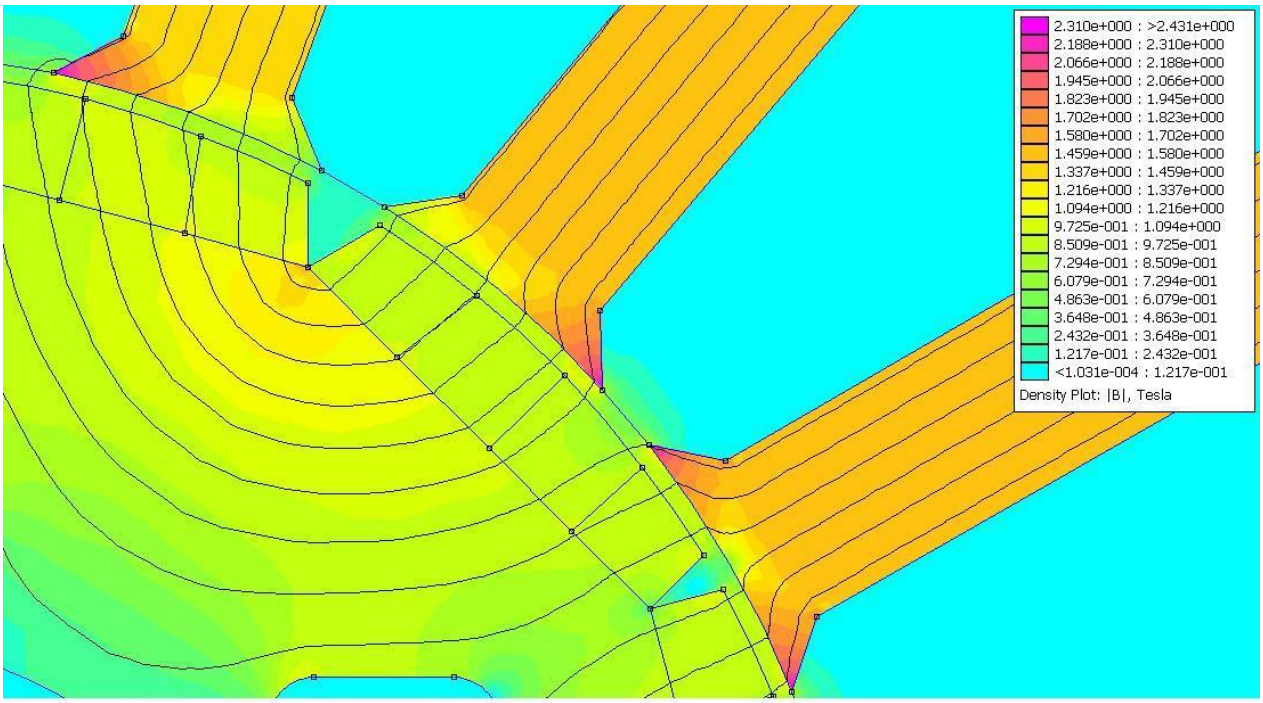

Fig. 11 Flux density plot in rotor, airgap and stator teeth

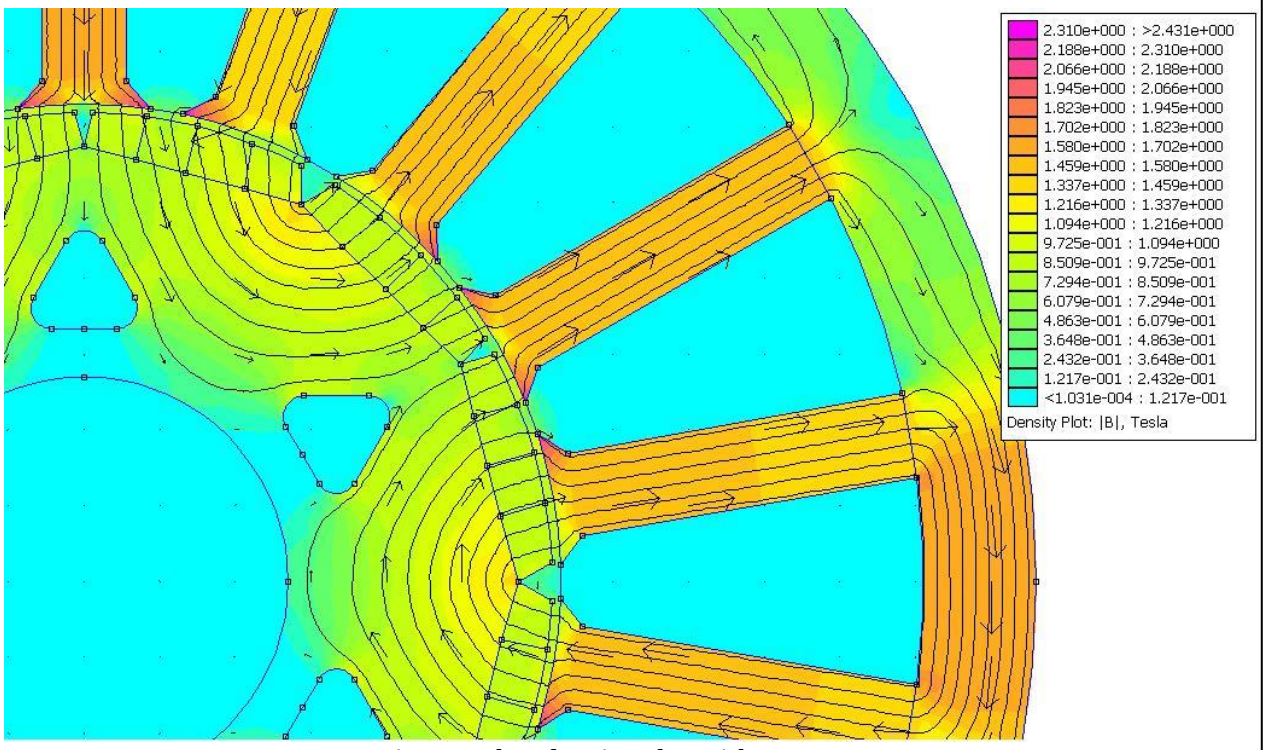

Fig. 12 Flux density plot with arrows

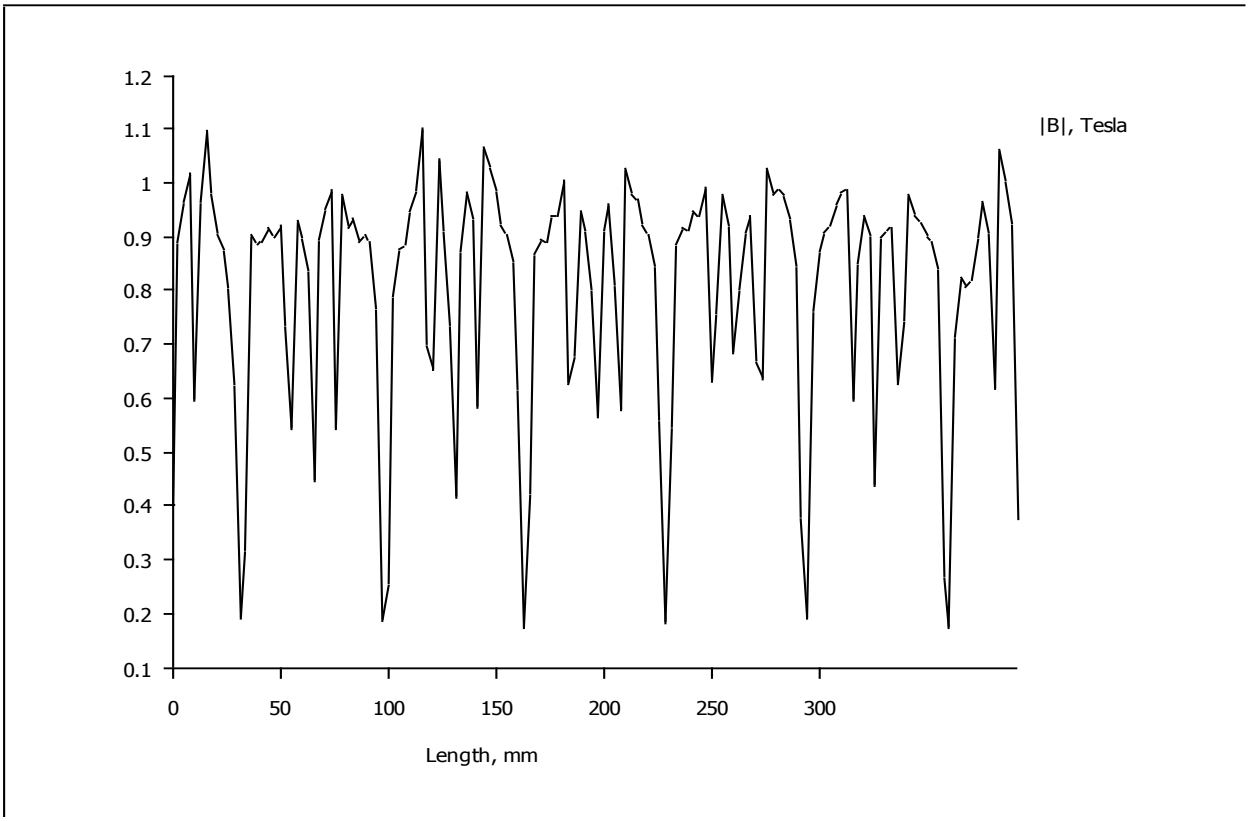

Fig. 13 Magnitude of the flux density in airgap without currents

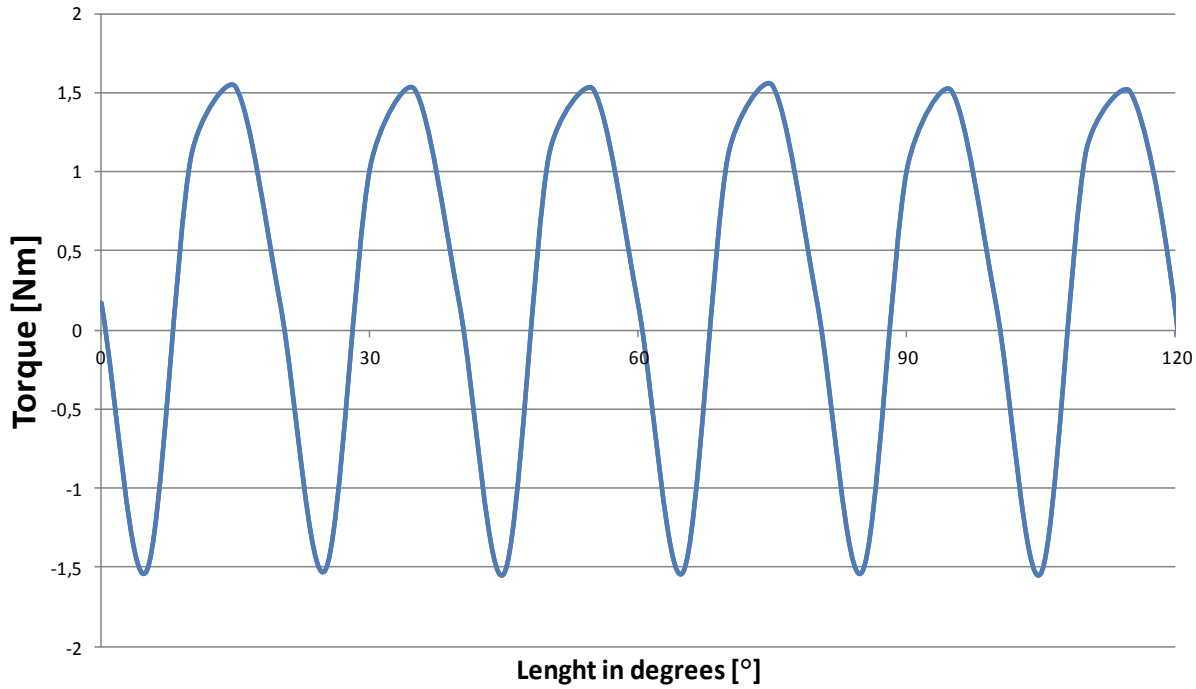

Fig. 14 The cogging torque of the synchronous machnine without currents in the stator windings

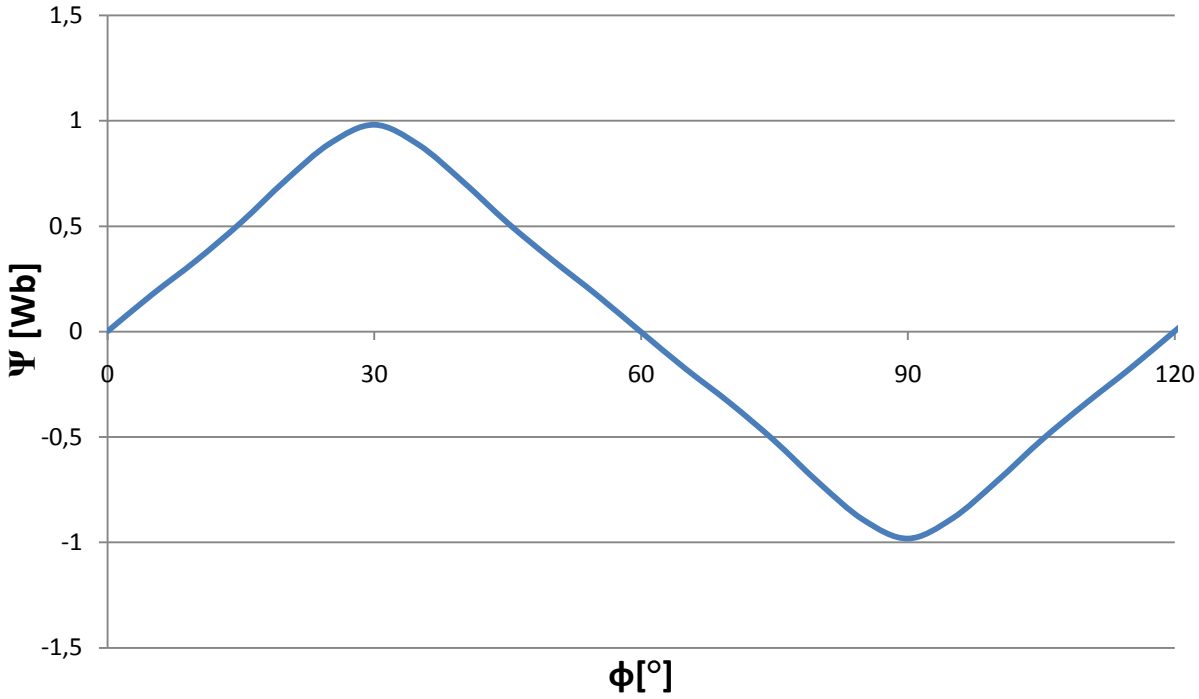

Fig. 15 Flux linkage in the airgap without currents in the stator windings

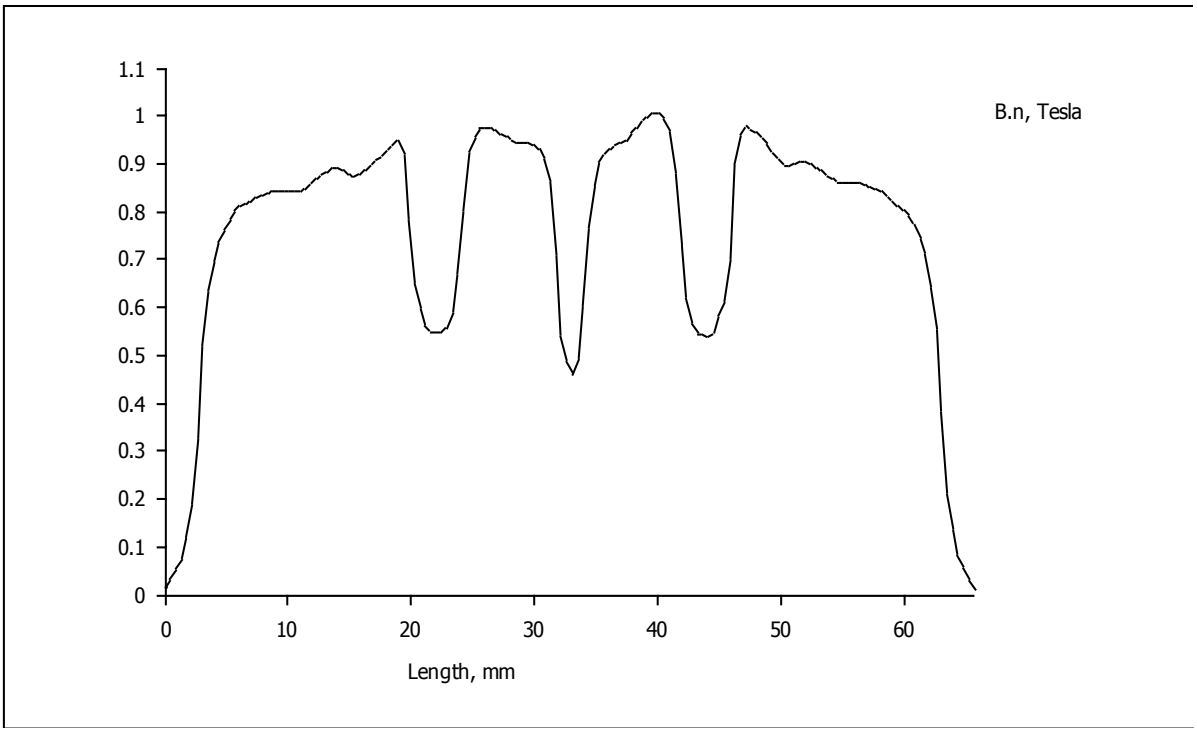

Fig. 16 Magnetic flux density over one pole

5.2 Simulation with currents

After familiarizing with the simulations without winding in the stator and with current 0 A in the stator windings, a complete simulation with currents is proceeded. Currents are set up to the windings in the stator to $\mathbf{I_a}$, $\mathbf{I_b}$, $\mathbf{I_c}$. From the analyse one can see how the magnetic flux lines changing in the machine with currents. Furthermore, from the simulation can be seen that the magnetic flux is also concentrating again to the teeth of the stator. The magnetic flux density in teeth is increasing to values around 1,59 T, or from value 1,4T to 1,71T. In the air gap the magnetic flux density is not increasing so much and it is moving around values 0,8 - 1,1 T, it could caused by the small current values in the stator because the accurate properties of the synchronous machine are not known, the calculations are only estimates. In the edges of the teeth oversaturating is occuring, where the magnetic flux density reaches values around 2,4 T. This value is too high for this machine and it is assumed by the author of ths work to be caused by sharp shaped teeth and its small surface and the representing currents in the stator winding. In graph on the Fig. 18. one can see how the magnetic flux density in air gap increased and changed.

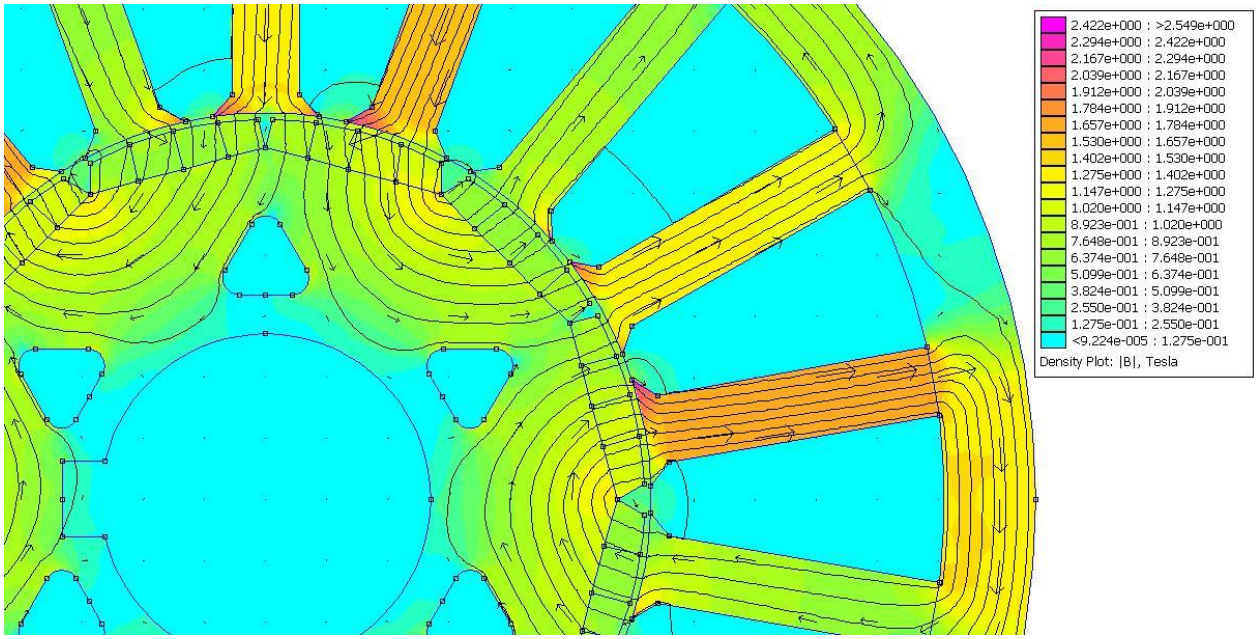

Fig. 17 Flux density plot with currents in windings

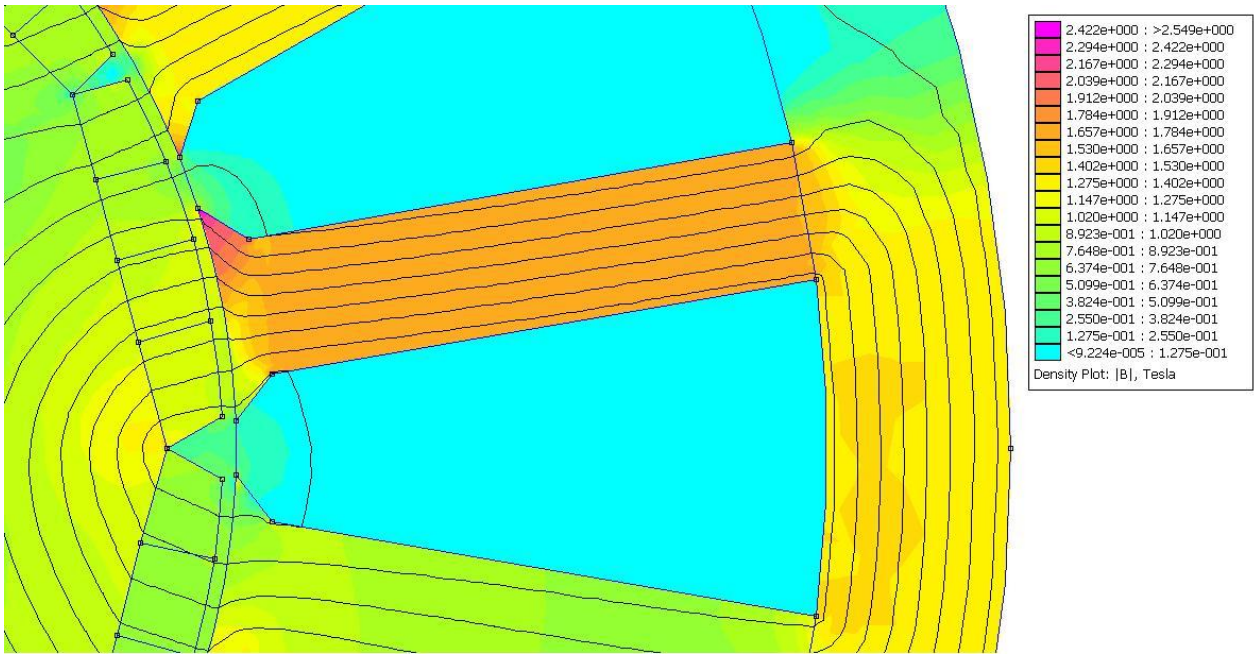

Fig. 18 Flux density in the airgap of the synchronous machine with currents in windings

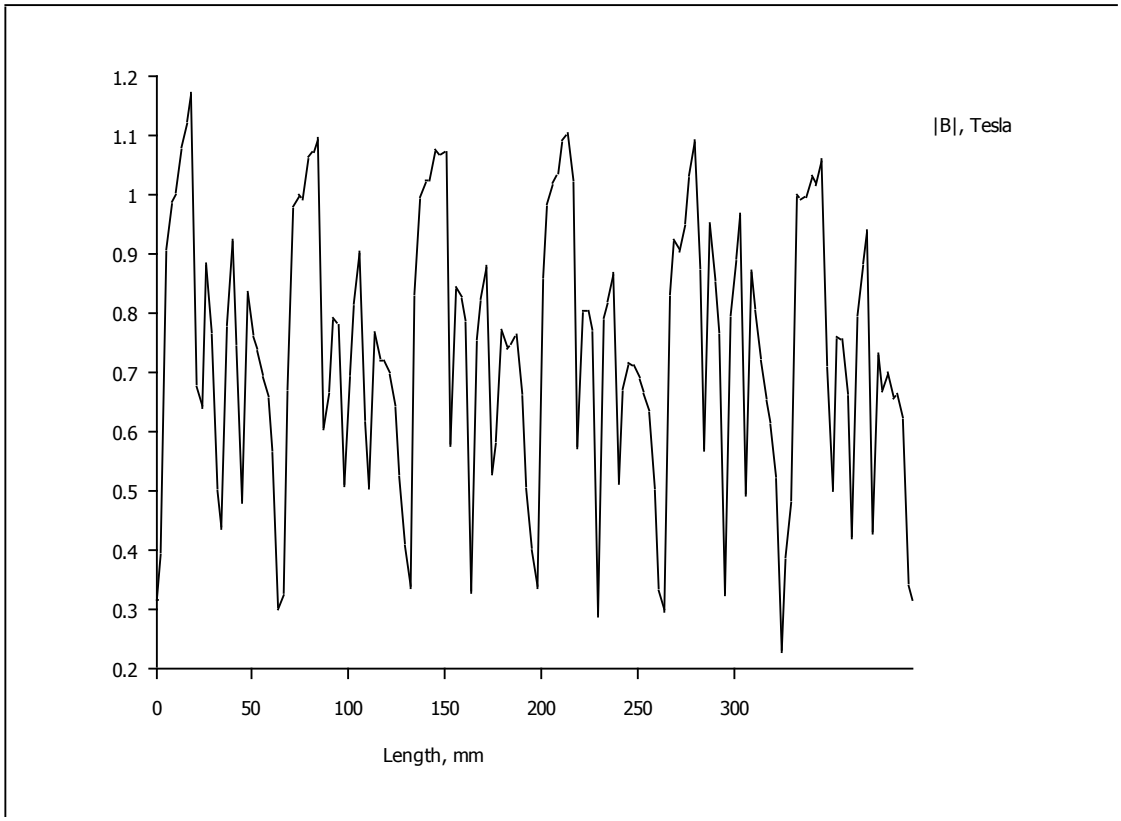

Fig. 19 Magnitude of the flux density in airgap with currents in windings

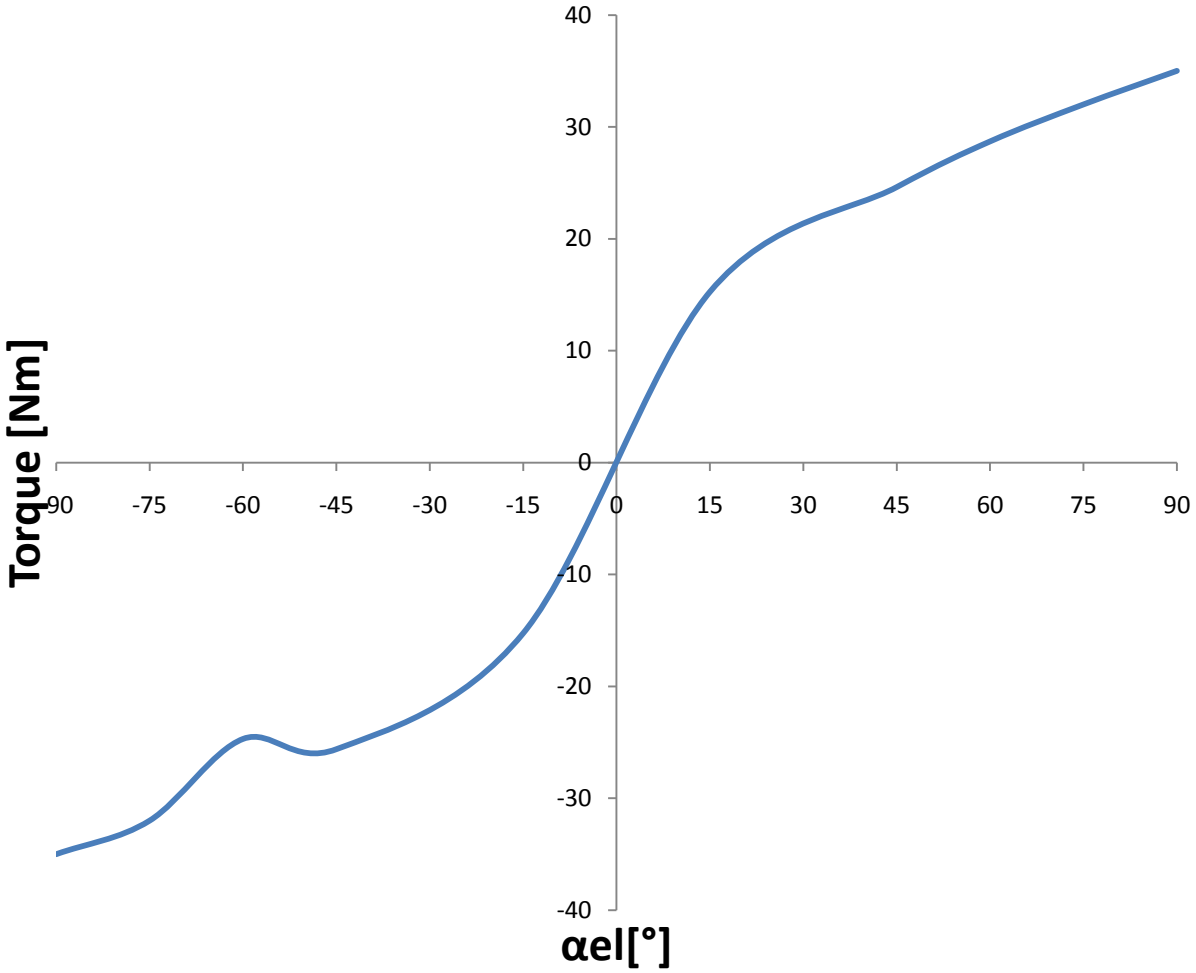

Fig. 20 Torque of the synchronous machine

6 ANIMATION

The animation and other data shown in figures of this work were made with function OctaveFEMM what is a Matlab toolbox that allows the operation of FEMM through a set of Matlab functions. The script is shown below:

```
echo on
path(path,'C:\Program Files\femm42\mfiles')
openfemm
main_maximize
opendocument('C:\ss_prud1_pre.FEM')
vystup=fopen('ssmoment_currents.txt', 'wt')
vystup1=fopen('fluxlinkage_currents1.txt', 'wt')
vystup2=fopen('fluxlinkage_currents2.txt', 'wt')
vystup3=fopen('fluxlinkage_currents3.txt', 'wt')
mi_seteditmode('group')
mi_zoomnatural
mi_maximize
pocet_prvkov=20
Alfa=-1
mi_analyse()
mi_loadsolution()
mo_showdensityplot(0,0,3,0,'mag')
mo_savebitmap(sprintf('spm_motor%1$d.bmp',i) )
N=mo_getcircuitproperties('Ia')
X=mo_getcircuitproperties('Ib')
Y=mo_getcircuitproperties('Ic')
fprintf(vystup1,'%12.8f %12.8f %12.8f \n',N)
fprintf(vystup2,'%12.8f %12.8f %12.8f \n',X)
fprintf(vystup3,'%12.8f %12.8f %12.8f \n',Y)
mo_seteditmode('area')
mo_groupselectblock(1)
M=mo_blockintegral(22)
fprintf(vystup,'%12.8f \n',M)
mo_close()
omega=2*pi*50
i=0
dt=0.00299
Im=6.4*0.707
 for i=1:pocet_prvkov
         ia=Im*sin(omega*i*dt)
         ib=Im*sin(omega*i*dt+((2*pi)/3))
         ic=Im*sin(omega*i*dt+((4*pi)/3))
         mi_modifycircprop('Ia',1,ia)
         mi_setcurrent('Ia',ia)
         mi_modifycircprop('Ib',1,ib)
```

```
            mi_setcurrent('Ib',ib)
            mi_modifycircprop('Ic',1,ic)
            mi_setcurrent('Ic',ic)

                  mi_selectgroup(1)
                  mi_selectgroup(2)
                  mi_moverotate(0,0,Alfa)
                  mi_analyse()
                  mi_loadsolution()
                  mo_showdensityplot(0,0,3,0,'mag')
                  mo_savebitmap(sprintf('ss_motor%1$d.bmp',i))
                  N=mo_getcircuitproperties('Ia')
                  X=mo_getcircuitproperties('Ib')
                  Y=mo_getcircuitproperties('Ic')
                  fprintf(vystup1,'%12.8f %12.8f %12.8f \n',N)
                  fprintf(vystup2,'%12.8f %12.8f %12.8f \n',X)
                  fprintf(vystup3,'%12.8f %12.8f %12.8f \n',Y)
                  mo_seteditmode('area')
                  mo_groupselectblock(1)
                  M=mo_blockintegral(22)
                  fprintf(vystup,'%12.8f \n',M)
                  mo_close()
i=i+1
end
  fclose(vystup)
```

7 ANSYS WORKBENCH

Appearance to that, the classical program Ansys is more likely destined to scientist and in common companies isn't possible to use effectively this program, the programmers create a new platform of Ansys. This version calls Ansys Workbench.

This program is focused on solving engineering problems from areas of physical fields and so on. As I noted previously, this new platform has better user interface and Workbench is able to solve all types of physical field like classical version, too. Some special functions are in this new interface subdued, but experienced user can use them with the help of commands and with language APDL.

One of the biggest advantages of this new platform is the easy work with geometry and with boundary conditions. Ansys Workbench is completed by new functions like automatic meshing tool, which is according to the scheduled problem can choose the right type and size of the elements. Of course there is possibility to define the mesh process. In version 11 is a new module, which can use experienced user to create manually the FEA mesh. So by these functions very good results in a short time are possible to obtain. So it is ideal tool for use in industry.

7.1 Designing the model

The model for analyzing in Ansys Workbench was created by parametric CAD system Autodesk Inventor. According to the graphical documentation a 3D model of the analyzed machine was created, but it was necessary to make certain simplification. Similarly as with model in my first semesteral thesis, where I was modeling 2D model with platform FEMM, complications with generating the mesh can occur, so it was more relevant in 3D model to delete the roundness and corner fillets. Due to this fact, the number of elements would rise and it could cause severity of solving the problem.

The model of the machine was imported from Autodesk Inventor to Ansys Workbench through format IGES, because other formats made deformations in the machine. The FEA mesh is creating with the help of automatic functions in Ansys Workbench. The user has only several chances to interfere the formation of the mathematical model. At automatic meshing is possible to set up several basic parameters. It is possible to set up the size and the dominant type of the elements in the volume of the model. The model used for simulation was completed about two volumes which are representing air, in and out of the motor. These volumes have the biggest count of elements of all models. To improve the quality of mesh mapped meshing was used on the surface of stator, so equal lay-out of elements was achieved. While setting up the conditions, a proper choice of the elements was taken into account, so the surface can be better described by the mesh with the expected magnetic inductance. On the other hand, there was an effort to make the mesh not so soft because the computation of the model could last much longer time. In the case of magnetic circuit of a synchronous machine it is necessary to increase the density of the mesh in places where the gradients of magnetic induction are big, like stator and rotor slots, the edges in air gaps, and air gaps as well. In the surface of the air gap, the size of the element was chosen in order to have 4 elements on the width of air gap. The area of air gap and the part of the iron is meshed by soft mesh so we get the necessary amount of data for the graph of distribution of magnetic induction in the air gap.

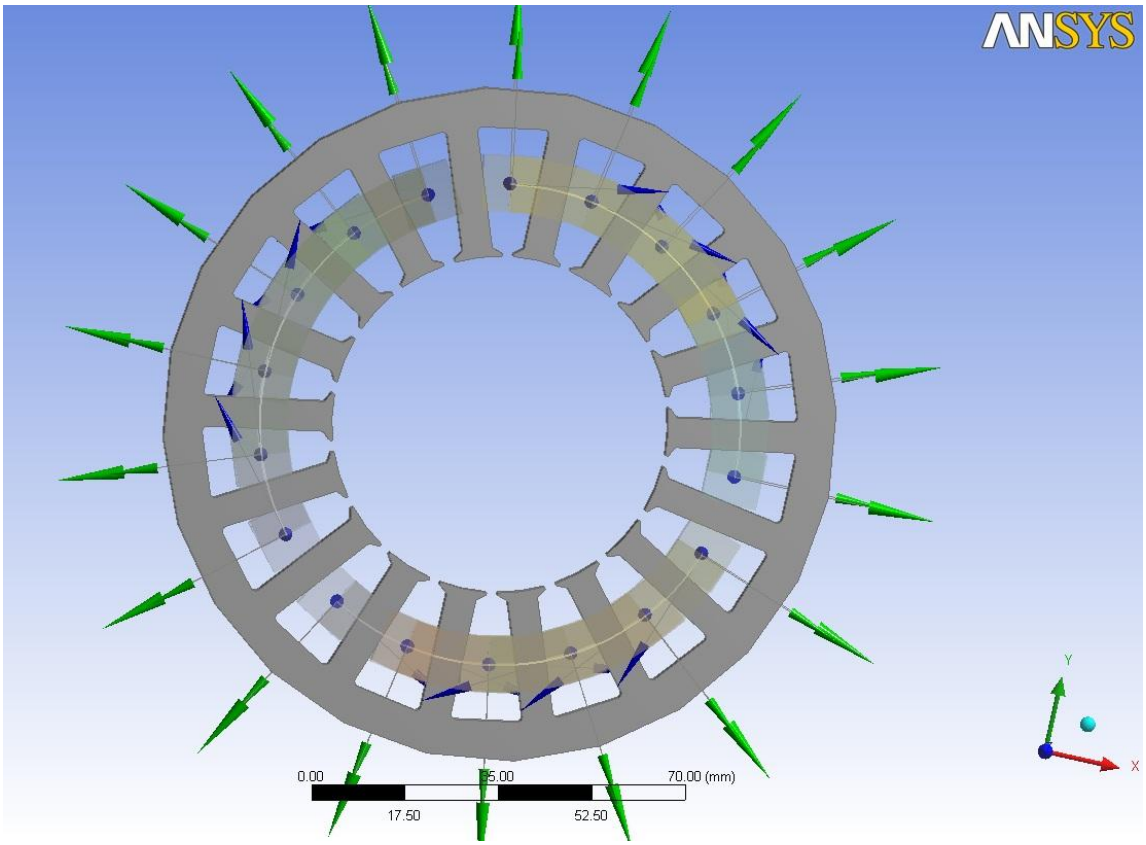

Fig. 21 - The stator winding in 3D model

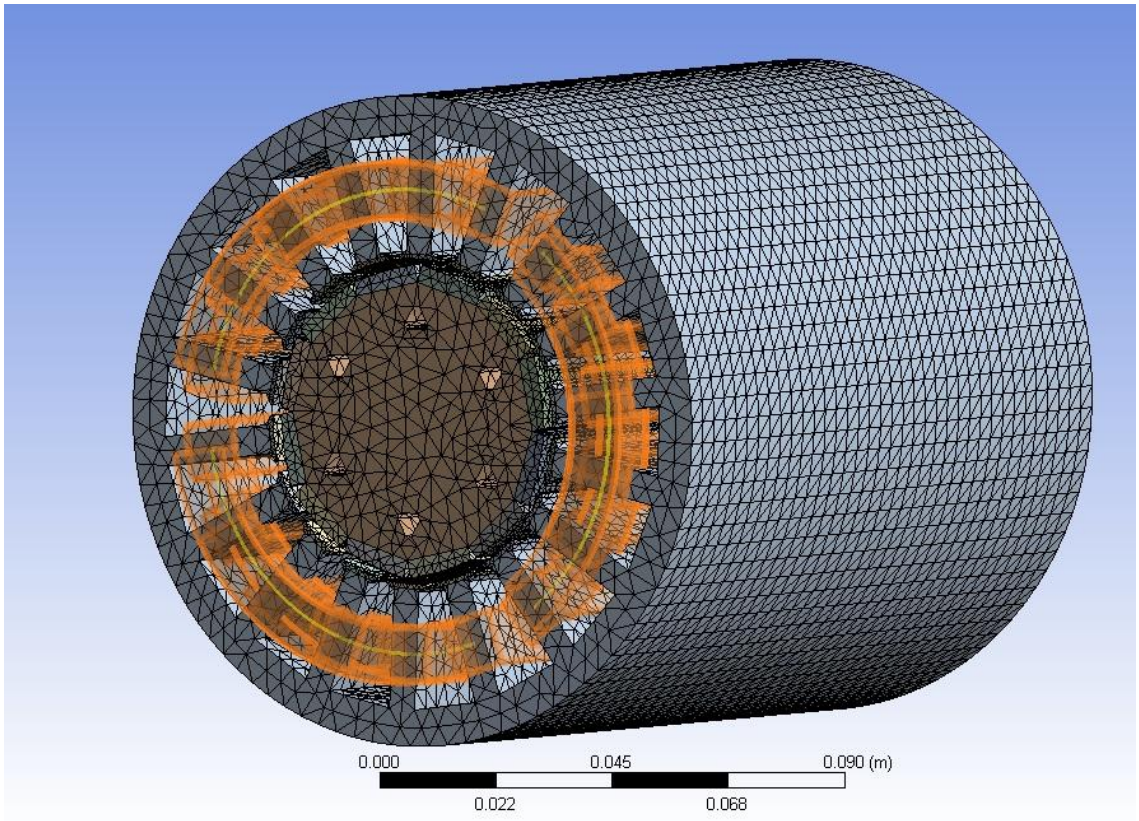

Fig. 22 The mesh elements in the 3D model

8 RESULTS OF THE SIMULATIONS

8.1 Simulation with the nominal current

First I have made simulation of the model with nominal currents, I=6A, in the stator windings. From the analyse, one can see how the magnetic flux density is changing in the machine. Furthermore, from the simulation also can be seen that the magnetic flux is concentrating to the teeth of the stator. The magnetic flux density in teeth achieving values around 1,4T, or from 0,6T to 1,46T. In the air gap the magnetic flux density moving aroun 0,7 T-1T. In the edges of the teeth we can remark occuring oversaturing where is the local maximum, magnetic flux density reaches values around 1,91 T . This value is caused by sharp shaped teeth and its small surface. On the Fig. 24. and 25. the change of the magnetic flux density on the bottom and in the edges of the stator tooth are shown. The minimum value is around 0,1 T and the maximum value moves around 1,4 T. This value can be considered as a normal for this type of machine.

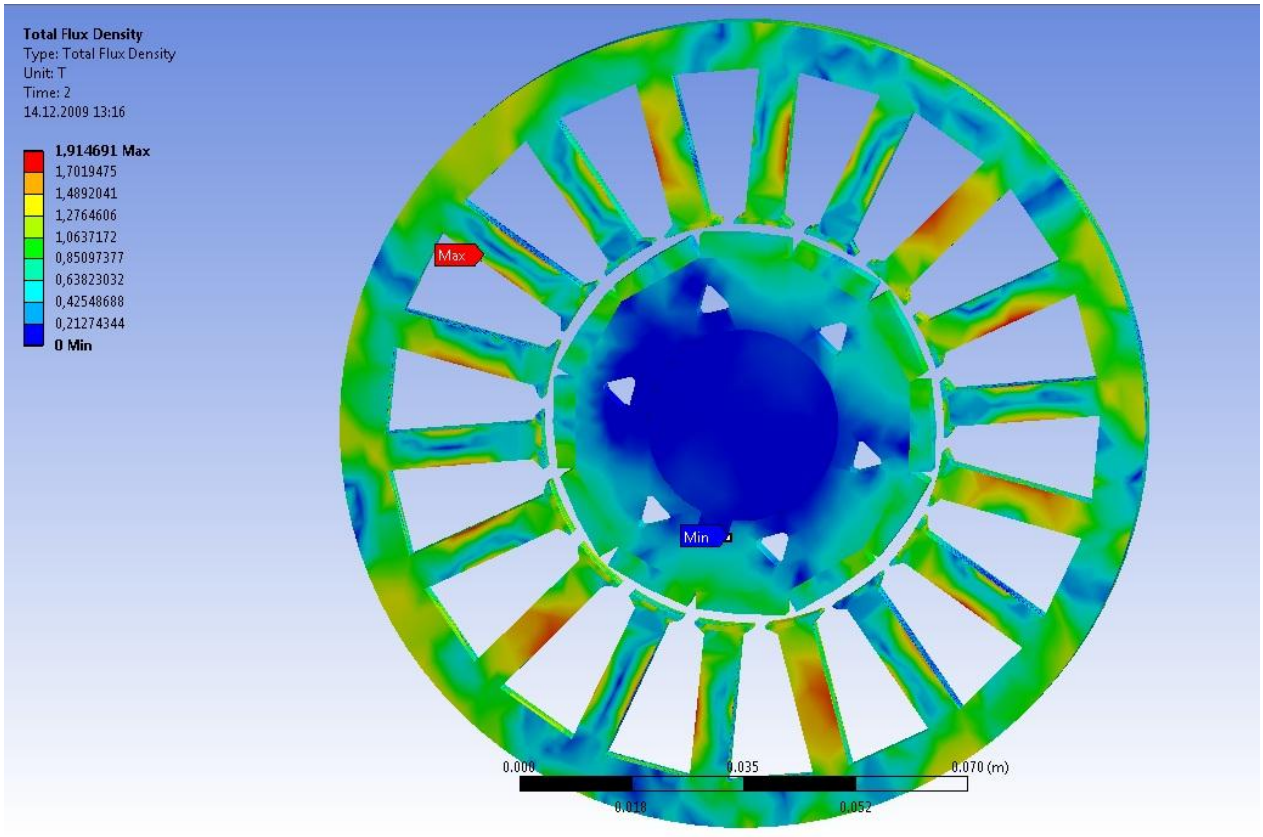

Fig. 23 Total flux density of the machine

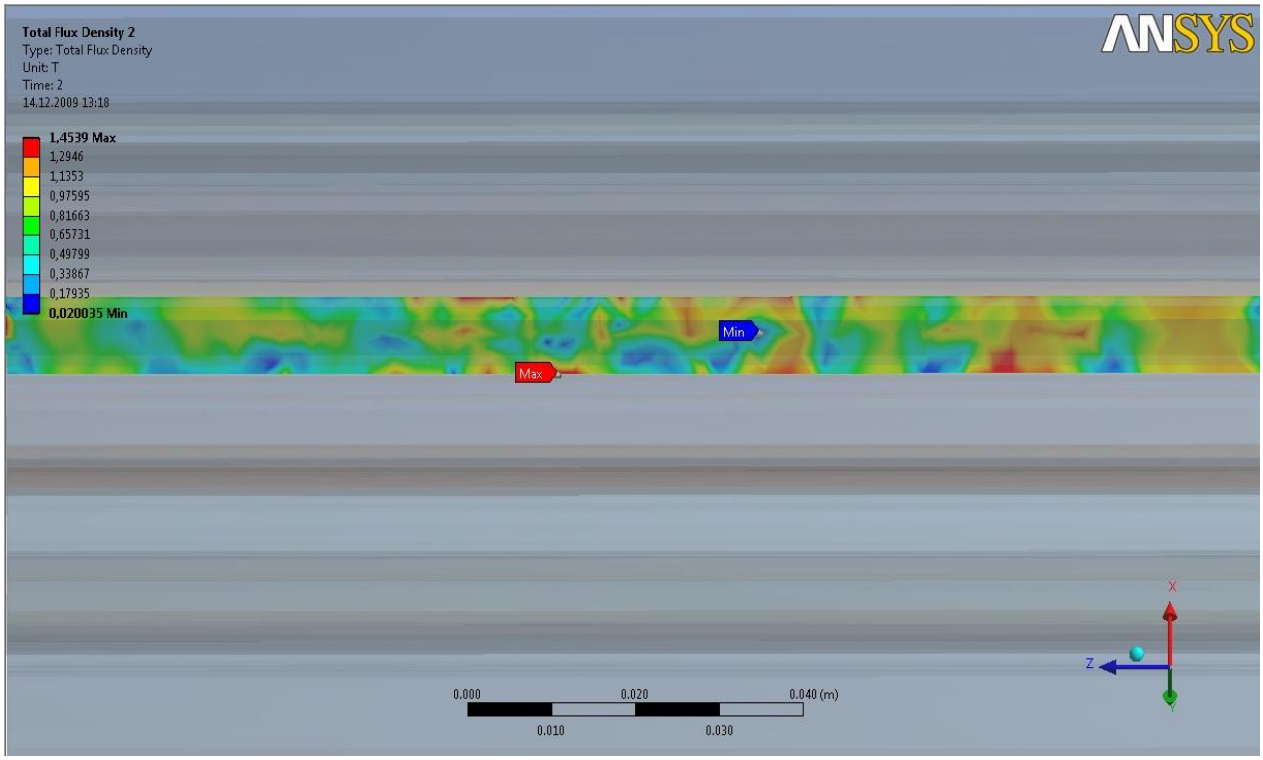

Fig. 24 Total flux density in the bottom of the stator tooth

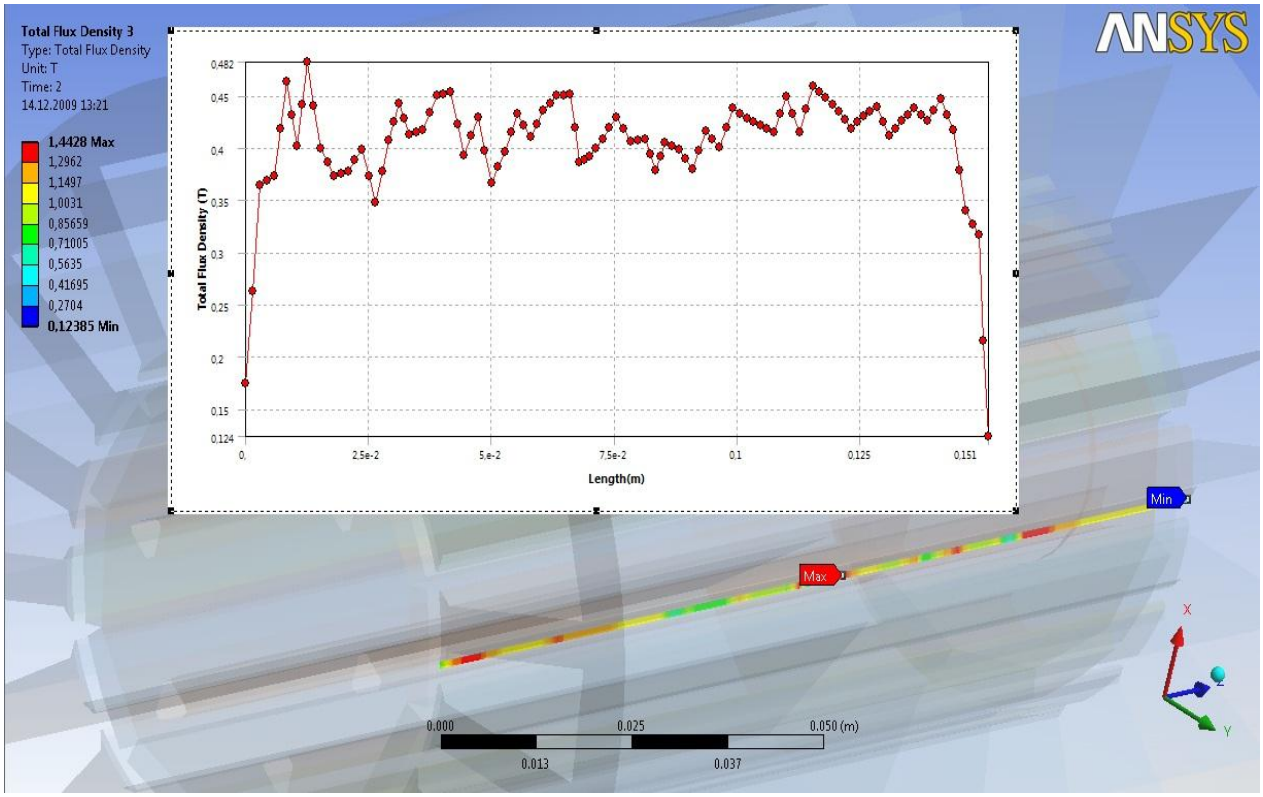

Fig. 25 The total flux density inthe edge of the stator teeth

8.2 Simulations with short circuit currents

After familiarizing with the simulations with the nominal current 6 A in the stator windings we proceed the complete simulation with higher, short-circuit stady-state currents after transient mode. Currents to values 25 A are set up, in the windings in the stator to $\boldsymbol{I_a}$, $\boldsymbol{I_b}$, $\boldsymbol{I_c}$. From the analyse it can be seen how the magnetic flux lines changing in the machine with higher currents. Furthermore, the simulation shows that the magnetic flux is also concentrating again to the teeth of the stator. The magnetic flux density in teeth is increasing to values around 1,707 T, or from value 1,2T to 2,19T. In the air gap the magnetic flux density did not increase much and it is moving around values 0,8 - 1,1 T. In the edges of the teeth oversaturating occurs, where the magnetic flux density reaches increasing to values around 2,19 T. This value is a little bit high value for this machine, but not as high as was in the simulation in program FEMM. We think it is also caused by sharp shaped teeth and its small surface as it was assumed and the representing currents in the stator winding is dangerous for this machine. The values on the bottom and on the edges of stator tooth was not raised dangerously.

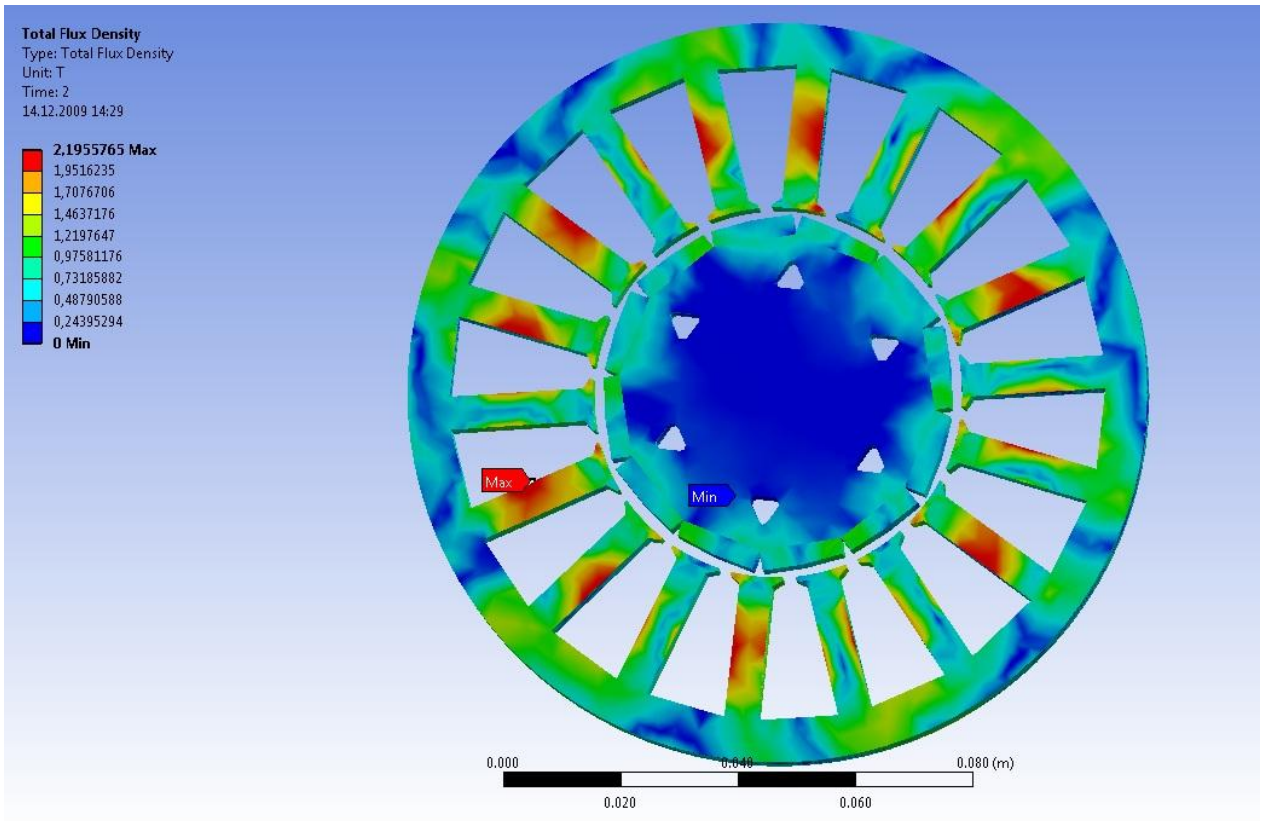

Fig. 26 Total flux density of the machine with short-circuit currents

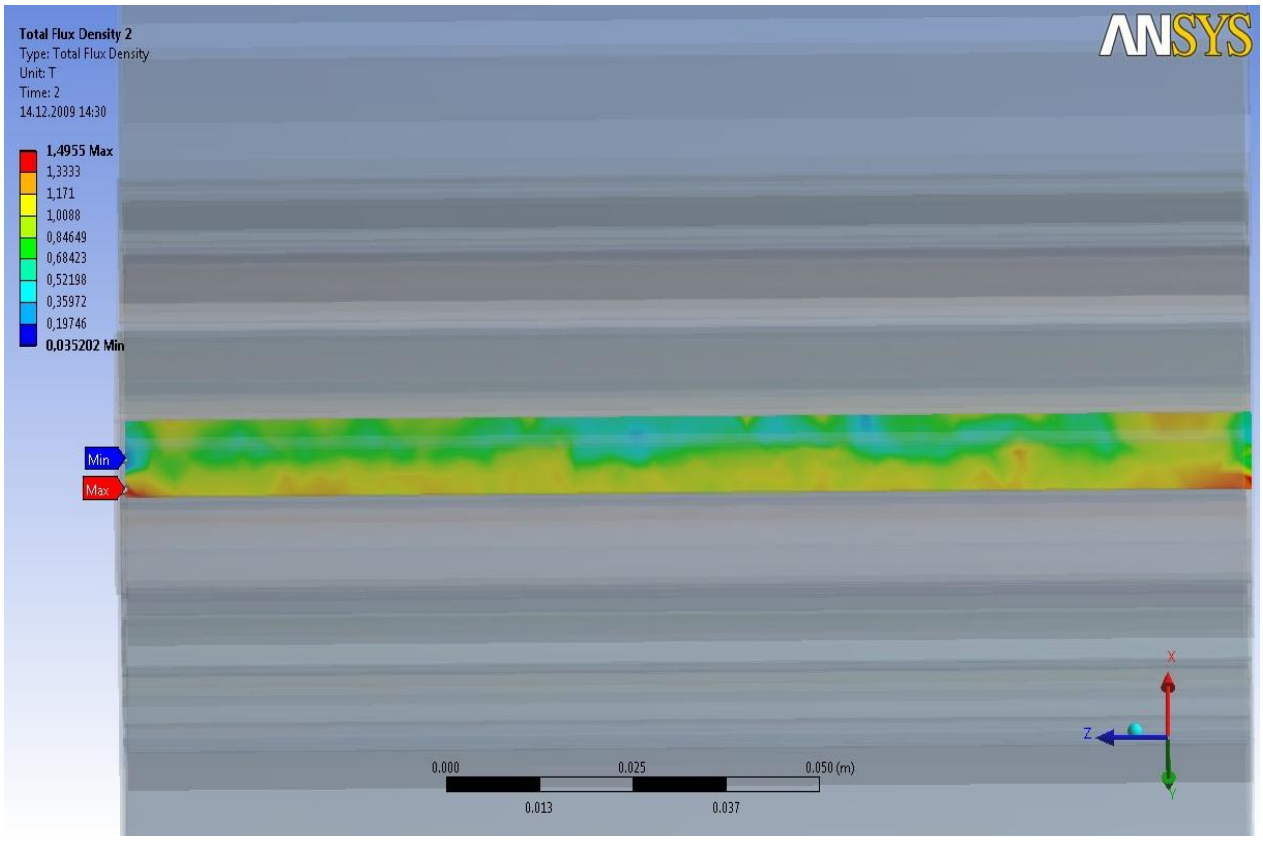

Fig. 27 Total flux density in the bottom of the stator tooth with short-circuit currents

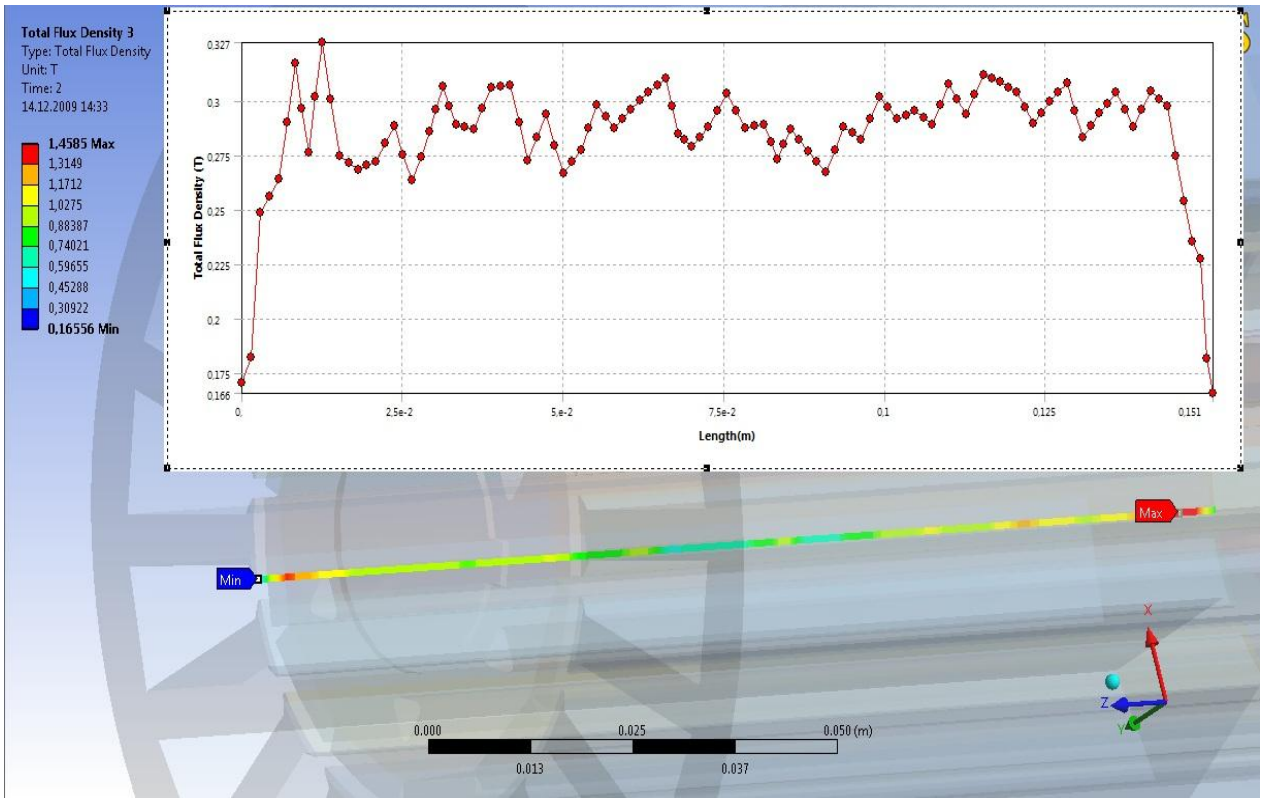

Fig. 28 The total flux density inthe edge of the stator teeth with short-circuit currents

9 CONCLUSION

Purpose of this thesis was to meet the distribution of the rotating magnetic field in synchronous machine with surfaced permanent magnets on its rotor. Calculating the critical parameters X_1 , X_a , X_s seemed a little complicated but the results dimensionally were correct. The engineered parameters of this machine are 1250 rpm, 60 Hz, and the synchronous reactance is 17Ω. Inaccuracy of the calculations may be caused by some parameters like frequency and synchronous speed were different and other parameters for calculating I chosed from tabular values. Using finite element method (FEA,FEM) with FEMM to model the functions of synchronous machine has shown as a fast and trustful method. Working with FEMM is as a whole, easy and simulating or modeling 2D models is adequate. Our 2D model in FEMM had about 76 000 elements. The results in air gap of the synchronous machine with PM are correct but in some places the value of the density is higher than in the real machines. This can be caused by sharp shaped teeth in small surface. In the second part of my work I made a 3D model in Ansys Workbench of the synchronous machine and it has shown as a very trustful method. Working with Ansys Workbench was not difficult and simulating 3D model is adequate. Comparing to FEMM, the model had about 450 000 elements and for magnetostatic simulations this value of elements is enough. The results of the total flux density in air gap of the SMPM was correct and in other places the value of the flux density was in normal range.

REFERENCES

[1] Juha Pyrhönen, Tapani Jokinen and Valéria Hrabovcova.: Desing of Rotating Electrical Machines. Finland 2008, ISBN: 978-0-470-69516-6

[2] Gől,O. Sobhi-Najafabadi,B.: A General Approach to the Dynamic Modelling of Permanent Magnet Machines. Mawson Lakes. Article.

[3] Jacek F. Gieras, Mitchell Wing.: Permanent Magnet Motor Technology. USA 2002, ISBN: 0-8247-0739-7.

[4] Ida, N. Bastos,J.P.A.: Electromagnetics and Calculation of Fields. New York:1992, ISBN: 0-387-97852-6.

[5] David Meeker, Ph.D.: FEMM Manual. Waltham